

Weak Gravitational Lensing Effects by Galaxy Clusters

Keiichi Umetsu (ASIAA)
with CLASH collaboration

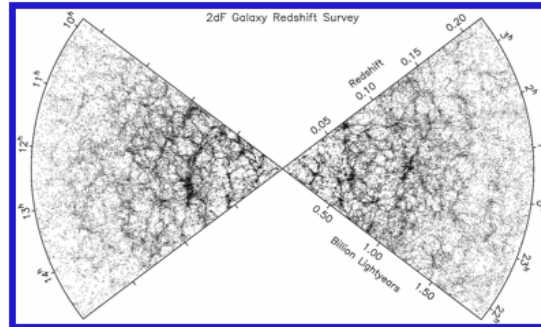
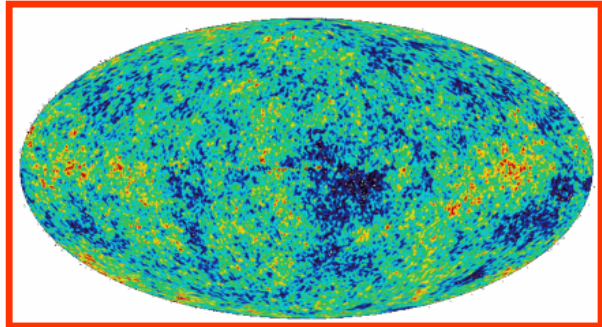


Introduction

Galaxy Clusters as Cosmological Probe

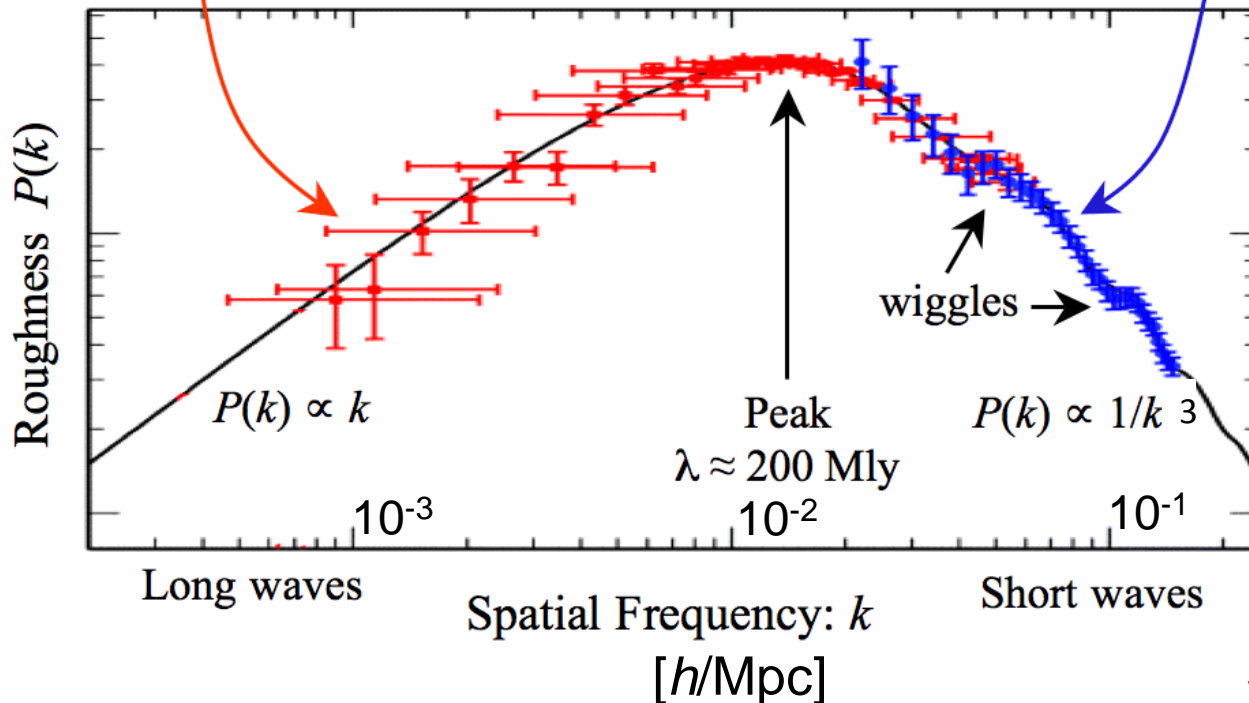
Λ CDM: Standard Structure Formation Paradigm

Matter power-spectrum density, $P(k)$



$$\delta := \frac{\rho - \bar{\rho}}{\bar{\rho}} = \frac{1}{(2\pi)^3} \int d^3k \tilde{\delta}(\mathbf{k}) e^{i\mathbf{k}\cdot\mathbf{x}}$$

$$\langle \tilde{\delta}(\mathbf{k}) \tilde{\delta}^*(\mathbf{k}') \rangle = (2\pi)^3 \delta_D^3(\mathbf{k} - \mathbf{k}') P(k)$$



$P(k) \propto k^{n_s}$ with $n_s \sim 1$ @ $k \ll k_{eq}$ (peak)

Turn-over @ $k \sim k_{eq}$

$P(k) \propto k^{(n_s-4)}$ @ $k \gg k_{eq}$

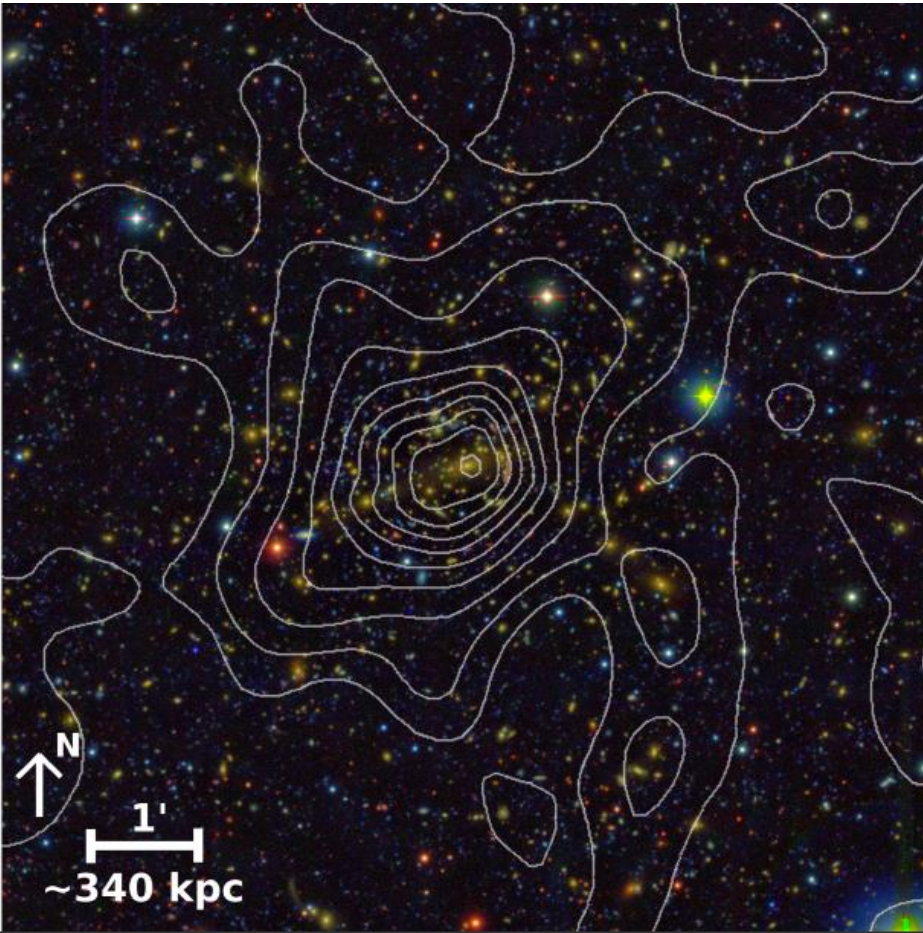
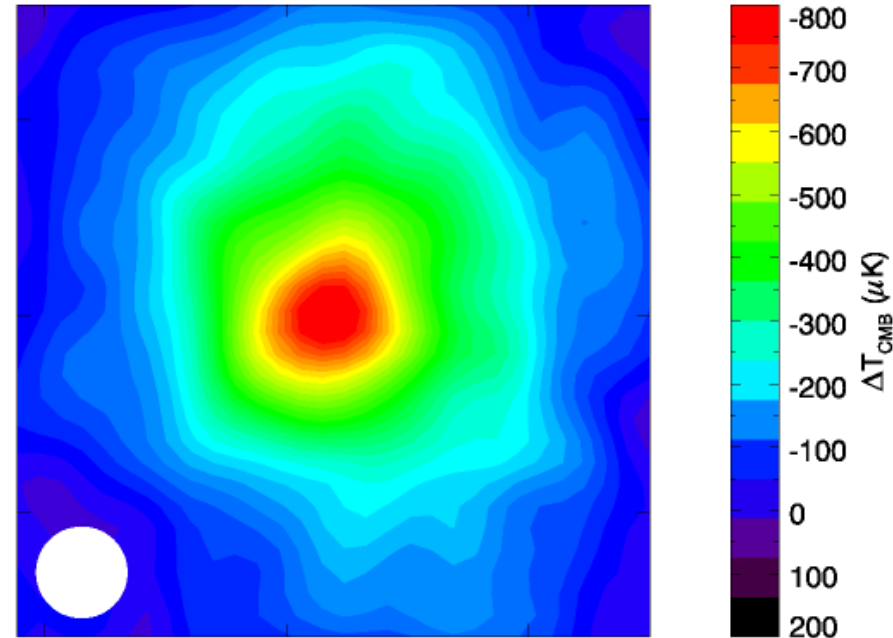
Nonlinear @ $k \gg 0.1 h/\text{Mpc}$

How about smaller scales, $\lambda < 10 \text{ Mpc}/h$?

Clusters of Galaxies

Clusters: the largest cosmic halos composed of 100-1000 galaxies.

Sunyaev-Zel'dovich Effect (SZE)



MACS1206 at $z=0.44$ (Umetsu et al. 2012)

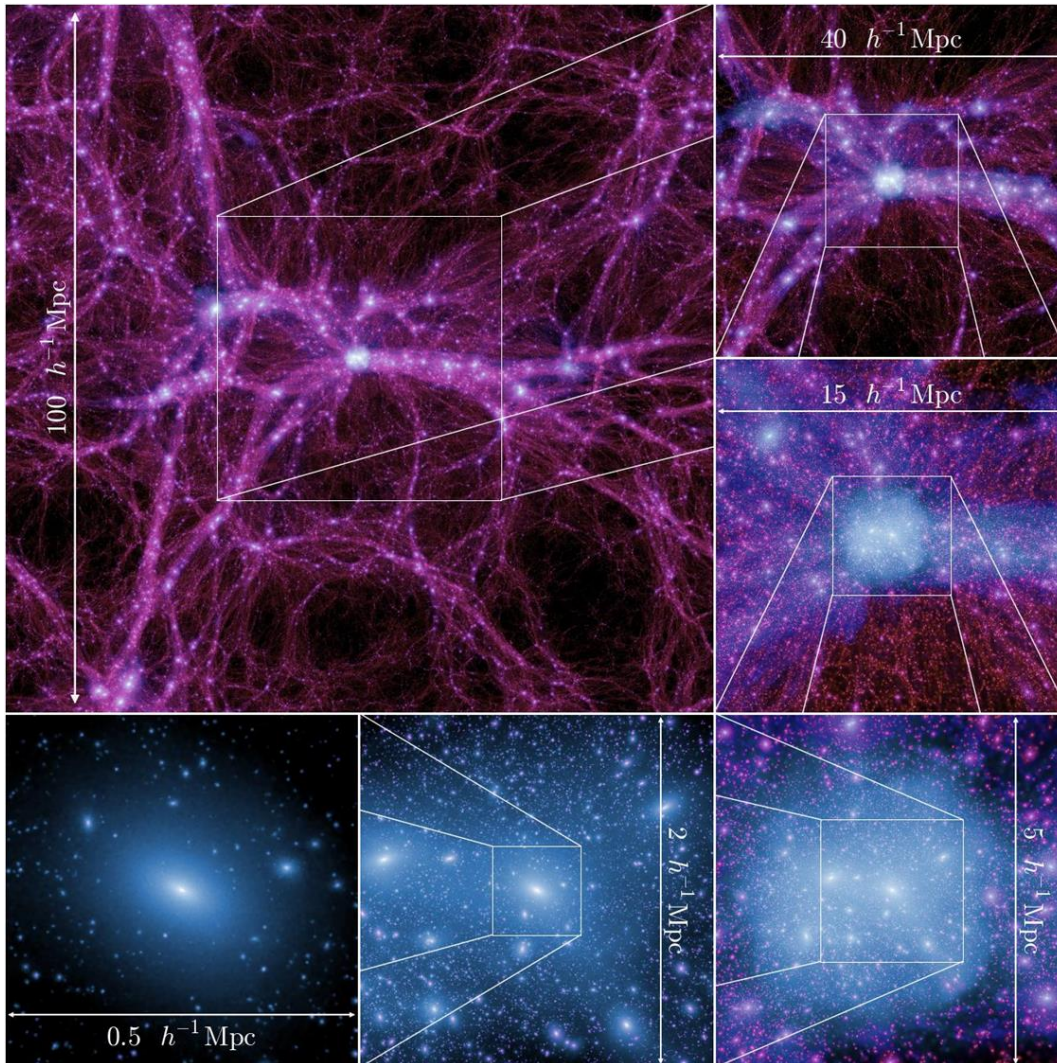
$$R_{\text{vir}} \sim 1-2 \text{ Mpc}$$

$$k_{\text{B}} T_{\text{gas}} \sim 3-10 \text{ keV}, \quad \sigma_v = 800-1300 \text{ km/s}$$

$$\Rightarrow M(R_{\text{vir}}) \sim 2R_{\text{vir}} \sigma_v^2 / G \sim 10^{14-15} M_{\text{sun}}$$

Clusters: the largest/youngest class of DM halos

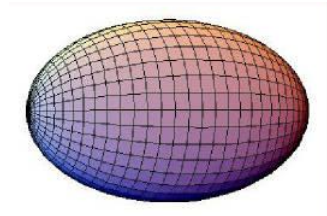
Halos = gravitationally-bound nonlinear objects



Typical formation epoch: $z_f=0.5-0.7$

Clusters formed at the intersection of filaments and sheets

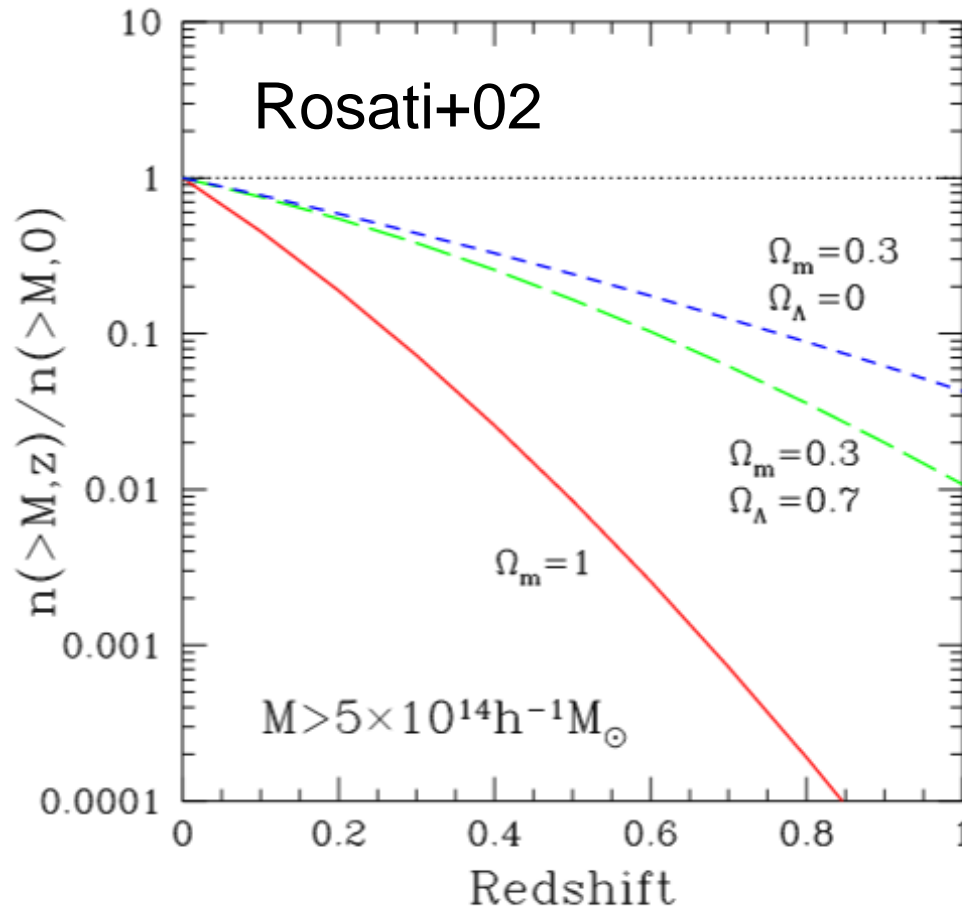
Halos are triaxial (collisionless nature)



Boylan-Kolchin+09

Clusters as Cosmological Probe

Cluster # counts $\frac{dN(> M_{\text{lim}}, z)}{d\Omega dz} = \int_{M_{\text{lim}}}^{\infty} dM \frac{dV(z)}{d\Omega dz} \frac{d^2 n}{dV dM}(M, z)$



Volume element

$$\frac{d^2 V}{dz d\Omega} = \frac{cr^2[\chi(z)]}{H(z)}, \quad \chi(z) = \int_0^z \frac{dz'}{H(z')}$$

Halo mass function

$$\frac{d^2 n}{dV dM}(M, z) \propto \exp\left[-\frac{v^2}{2}\right]$$

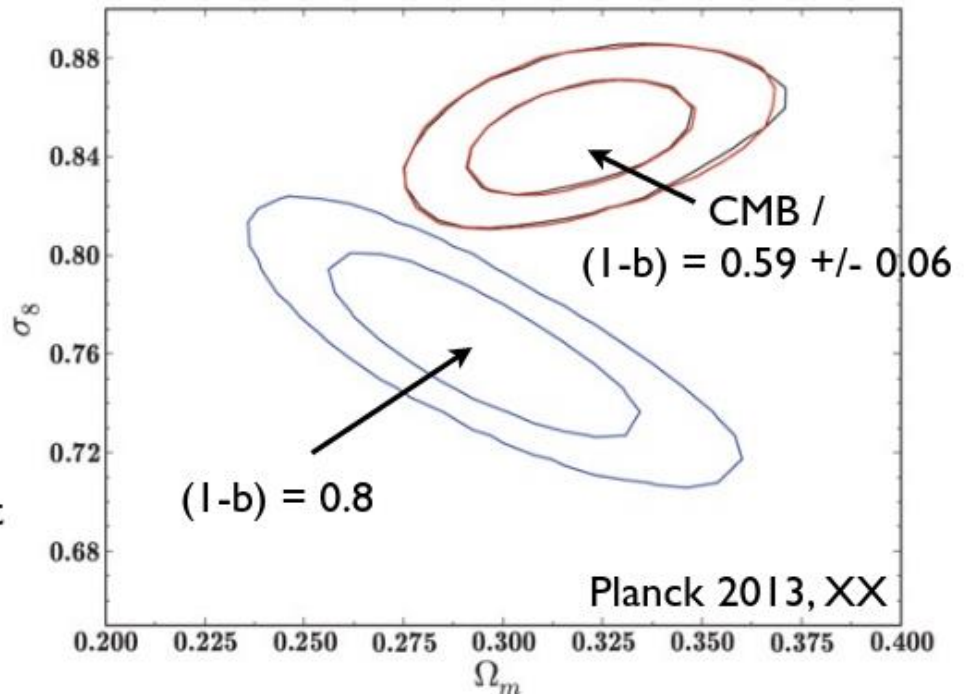
$$v \equiv \frac{\delta_c}{\sigma(M, z)} = \frac{\delta_c}{D_+(z)\sigma(M, 0)} \sim 3 \text{ for clusters}$$

Cluster counts are exponentially sensitive to *cosmology* and **cluster mass calibration!**

Planck CMB vs. SZE-Cluster Cosmology

$b=0.2?? - 0.4??$

- Planck: 3σ tension between SZ cluster counts and CMB cosmology
- assumes $M_{\text{Planck}} / M_{\text{true}} = (1-b) = 0.8$
- calibrated with XMM hydrostatic masses (Arnaud et al. 2010) + simulations



suggested explanations:

- **mass bias underestimated** (and no accounting for uncertainties)
- 2.9σ detection of neutrino masses: $\Sigma m_\nu = (0.58 \pm 0.20) \text{ eV}$
(Planck+WMAPpol+ACT+BAO: $\Sigma m_\nu < 0.23 \text{ eV}$, 95% CL)

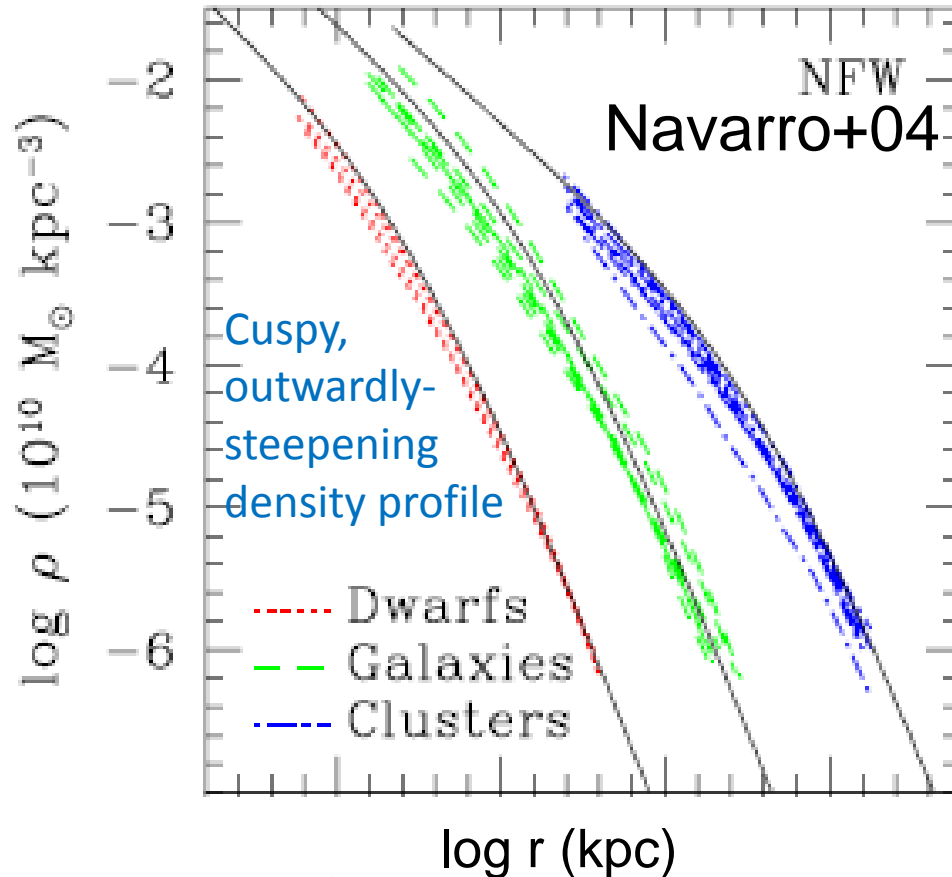
Slide taken from Anja von der Linden's presentation

Key Predictions of nonlinear structure formation models

(1) Quasi self-similar DM-halo density profiles

Quasi Self-similar Halo Density Profile for collisionless CDM

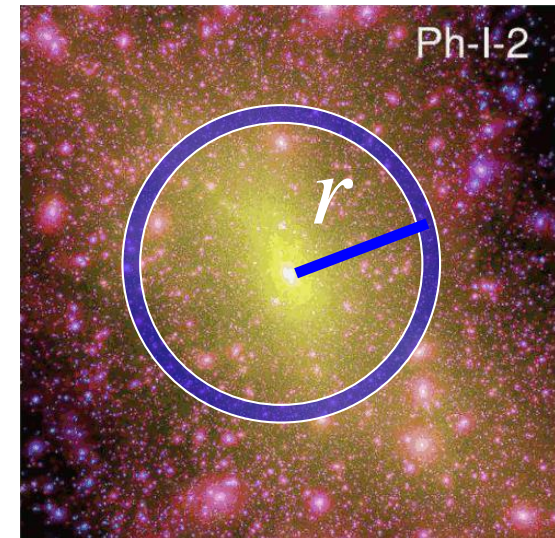
Spherically-averaged DM density profiles $\langle\rho(r)\rangle$ from numerical simulations



Empirical fitting formula by Navarro-Frenk-White (NFW)

$$\begin{aligned}\rho(r) &= Af(r/r_s) \\ &= \frac{\rho_s}{(r/r_s)(1+r/r_s)^2}\end{aligned}$$

Final products of nonlinear gravitational physics: nearly independent of halo mass, redshift, initial conditions, and cosmology

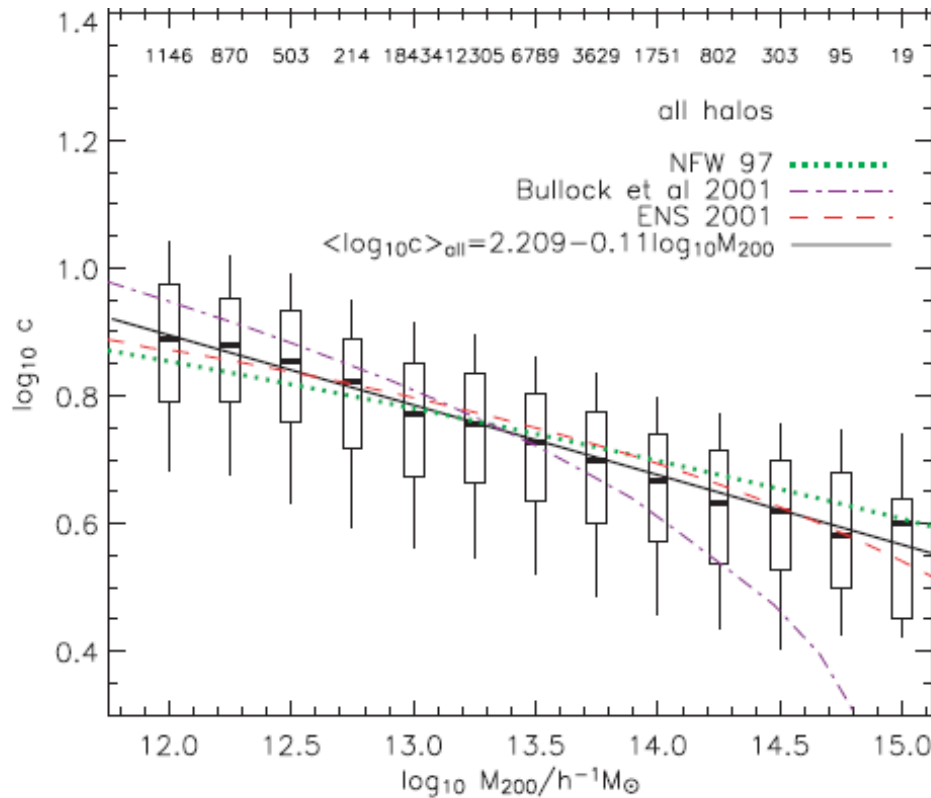


Key Predictions of nonlinear structure formation models

(2) Halo concentration-mass relation

Degree of Mass Concentration

$$c_{200} \equiv \frac{r_{200}}{r_s} = \frac{\text{Virial radius}}{\text{Isothermal (scale) radius}}$$



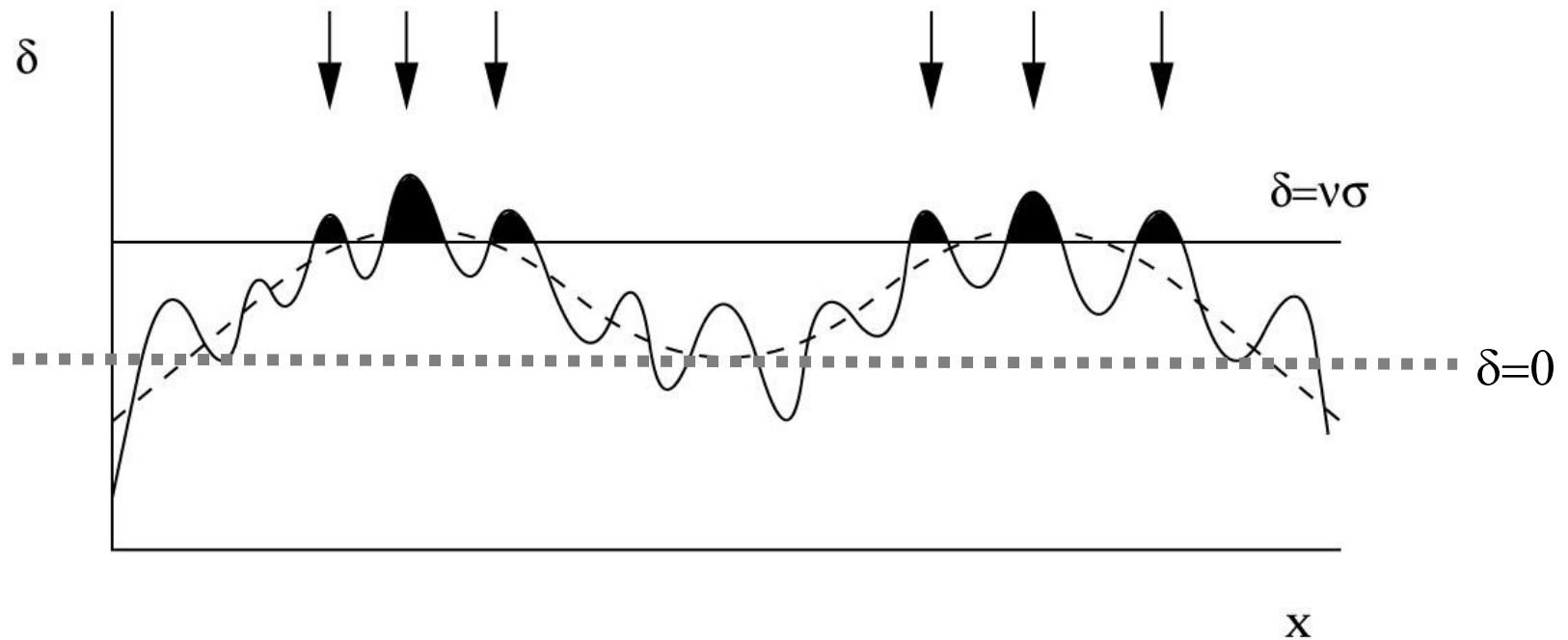
In hierarchical structure formation, $\langle c \rangle$ is predicted to decrease with increasing M

DM halos that are more massive collapse later on average, when the mean background density of the universe is correspondingly lower (Bullock+01; Neto+07)

Clusters (groups) of galaxies are predicted to have $\langle c_{200c} \rangle = 3-4$ (5-6) (Duffy+08; Bhattacharya+13)

Key Predictions of nonlinear structure formation models

(3) Halo bias: surrounding large-scale structure

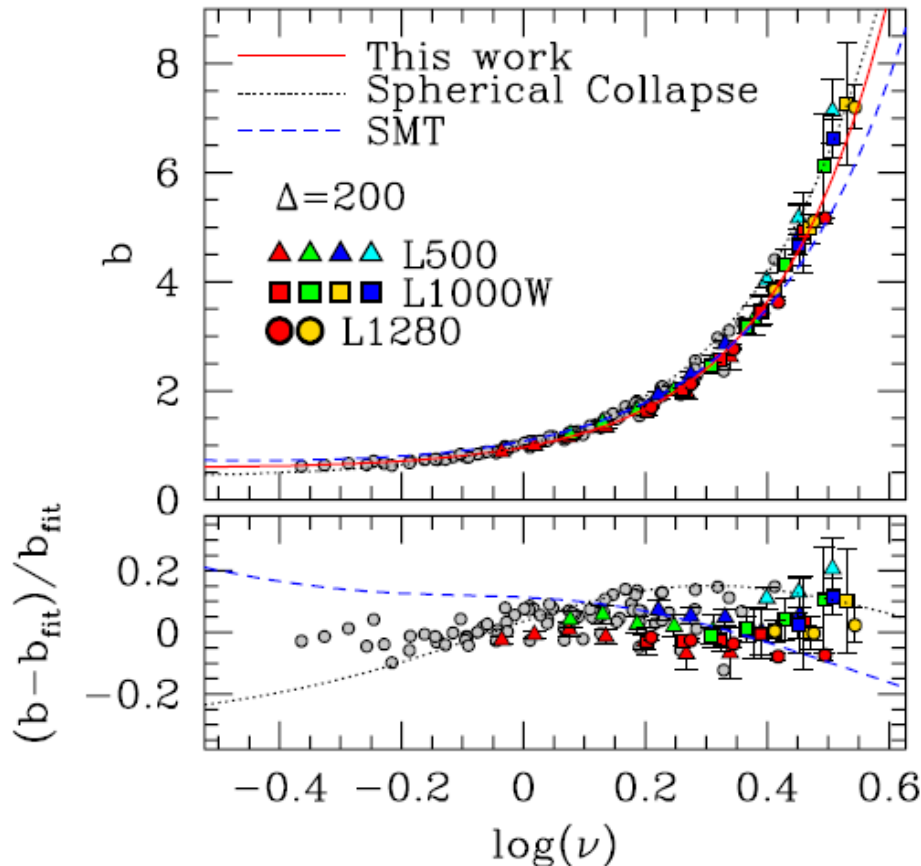


Halo Bias Factor: $b_h(M, z)$

2h term

Clustering of matter
around halos with M:

$$\xi_{\text{hm}}(r | M) = \frac{\langle \rho_{1\text{h}}(r | M) \rangle}{\bar{\rho}} + b_h(M) \xi_{\text{mm}}(r)$$



$$b_h(\nu) \approx 1 + \frac{\nu^2 - 1}{\delta_c}$$

$$\nu \equiv \frac{\delta_c}{\sigma(M, z)} \sim 3 - 4 \text{ for clusters}$$

$$(\log_{10} \nu \sim 0.5 - 0.6)$$

Tinker+10 LCDM simulations

My Approach: Weak Lensing

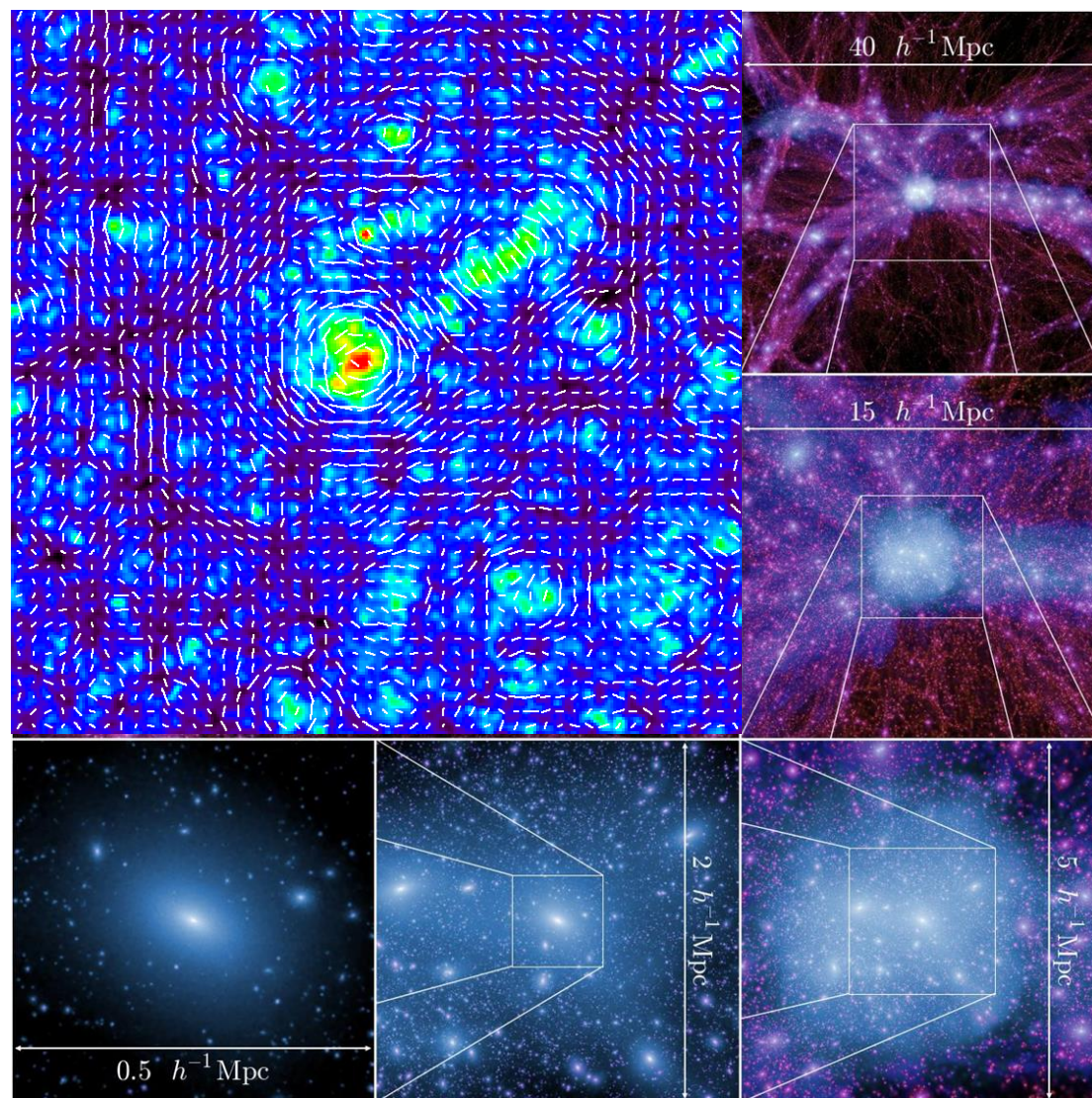
Objectives

Halo structure (1h)

- ✓ *Virial mass, M_{200} :*
- ✓ *Halo density profile, $\langle \rho(r) \rangle$:*
- ✓ *Mass concentration, $c(M,z)$:*

Surrounding LSS (2h)

- ✓ *Halo bias $b(M,z)$*
- ✓ *Primordial matter $P(k)$*



Weak Gravitational Lensing by Galaxy Clusters

Gravitational Bending of Light

Light rays propagating in an inhomogeneous universe will undergo **small transverse excursions** along the photon path

FLRW metric perturbed with Ψ

$$ds^2 = a^2(\eta)d\tilde{s}^2 = a^2\tilde{g}_{\mu\nu}dx^\mu dx^\nu$$

$$= a^2 \left[-(1 + 2\Psi)d\eta^2 + (1 - 2\Psi) \left\{ d\chi^2 + r^2(\chi)(d\theta^2 + \sin^2\theta d\phi^2) \right\} \right]$$

Bending angle: small transverse excursion of photon momentum ($|\Phi|/c^2 \ll 1$)

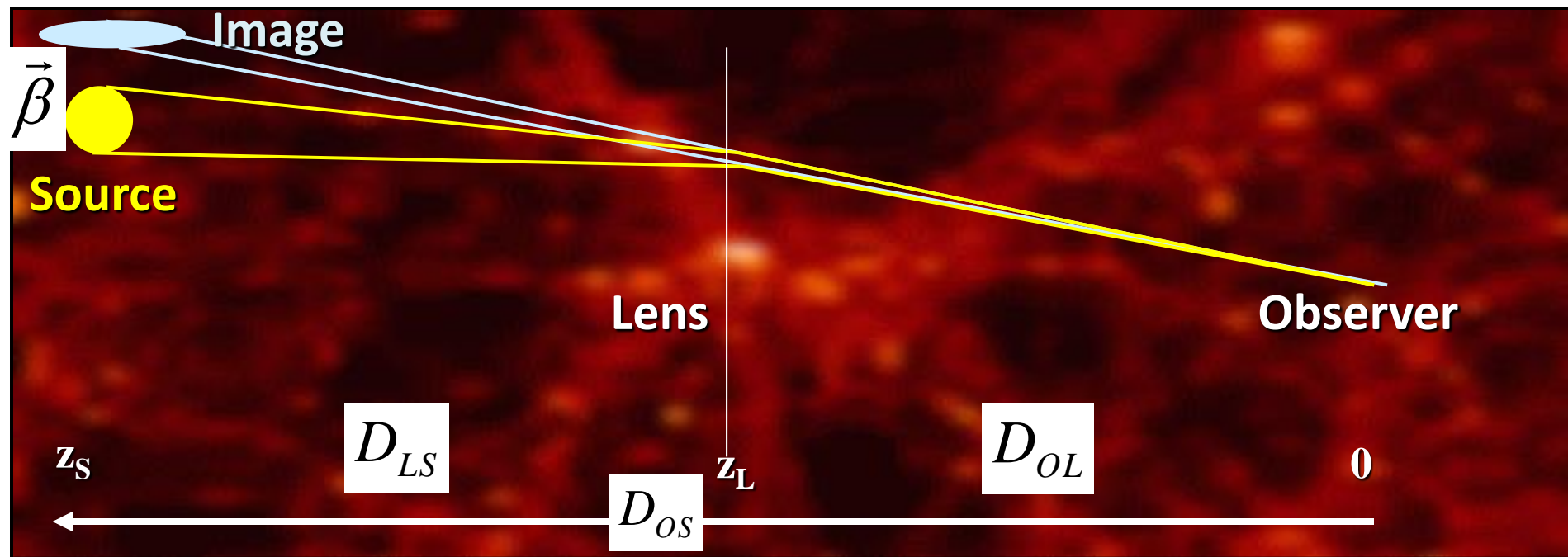
$$\delta\hat{\alpha} \approx \frac{\delta p_\perp}{p_\parallel} = -\frac{2}{c^2} \underbrace{\nabla_\perp \Psi(\chi_\parallel, \chi_\perp)}_{\text{Gravitational field of deflecting matter}} \delta\chi_\parallel$$

Gravitational field of deflecting matter

$$\hat{\alpha}^{\text{GR}} = 2\hat{\alpha}^{\text{Newton}} \rightarrow \frac{4GM}{c^2 r} = 1.75 \left(\frac{M}{M_{\text{sun}}} \right) \left(\frac{r}{R_{\text{sun}}} \right)^{-1}$$

Gravitational Deflection and Distortion

$\vec{\theta}$ **Lens Equation:** $\beta(\theta) - \theta = \frac{D_{LS}}{D_{OS}} \int_{\text{Observer}}^{\text{Source}} \delta\hat{\alpha}(\theta) \equiv -\nabla\psi(\theta)$



Deformation of an image

$$\delta\beta_i = (\delta_{ij} - \psi_{,ij})\delta\theta_j + O(\delta\theta^2)$$

Magnification, μ

$$\mu^{-1} = \det\left(\frac{\partial\beta}{\partial\theta}\right) = |1 - \nabla\nabla\psi|$$

Lensing Convergence, κ

κ : weighted line-of-sight projection of density contrast $\delta = \delta\rho/\rho$

$$\kappa = \frac{3H_0^2\Omega_m}{2c^2} \int_0^{\chi_s} d\chi \frac{r(\chi)r(\chi_s - \chi)}{r(\chi_s)} \frac{\delta}{a} = \int_{\text{Observer}}^{\text{Source}} d\Sigma \Sigma_{\text{crit}}^{-1}$$

Projected mass density field

$$\Sigma(\chi_{\perp}) = \int_0^{\chi_s} d\chi a(\rho - \bar{\rho}) = \int_{\text{Observer}}^{\text{Source}} dl \delta\rho$$

Critical surface mass density for lensing

$$\Sigma_{\text{crit}} = \frac{c^2}{4\pi G} \frac{D_{\text{OS}}}{D_{\text{OL}}D_{\text{LS}}}$$

- **Strong lensing:** $\Sigma \sim \Sigma_{\text{crit}}$ @ cluster cores
- **Weak lensing:** $\Sigma \sim 0.1 \Sigma_{\text{crit}}$ @ outside cores
- **Cosmic lensing:** $|\Sigma| < \sim 0.01 \Sigma_{\text{crit}}$ @ LSS

2D Poisson Equation

Effective lensing potential

$$\psi(\boldsymbol{\chi}_\perp) \equiv \frac{2}{c^2} \frac{D_{\text{LS}}}{D_{\text{OL}} D_{\text{OS}}} \int_0^{\chi_s} \Psi(\chi, \boldsymbol{\chi}_\perp) d\chi$$

2D Poisson eq. & Deflection field

$$\begin{aligned} \kappa(\boldsymbol{\chi}_\perp) &= -\text{div} \boldsymbol{\alpha} = \frac{1}{2} \Delta_\perp \psi(\boldsymbol{\chi}_\perp) \\ \boldsymbol{\alpha}(\boldsymbol{\chi}_\perp) &\equiv -\nabla_\perp \psi = -\frac{2}{c^2} \frac{D_{\text{LS}}}{D_{\text{OS}}} \int_0^{\chi_s} \nabla_\perp \Psi(\chi, \boldsymbol{\chi}_\perp) d\chi \end{aligned}$$

Cosmological 3D Poisson eq.

$$\begin{aligned} \Delta \Psi(\boldsymbol{\chi}) &= 4\pi G \bar{\rho} a^2 \delta \\ &= \frac{3}{2} H_0^2 \Omega_m \frac{\delta}{a} \end{aligned}$$

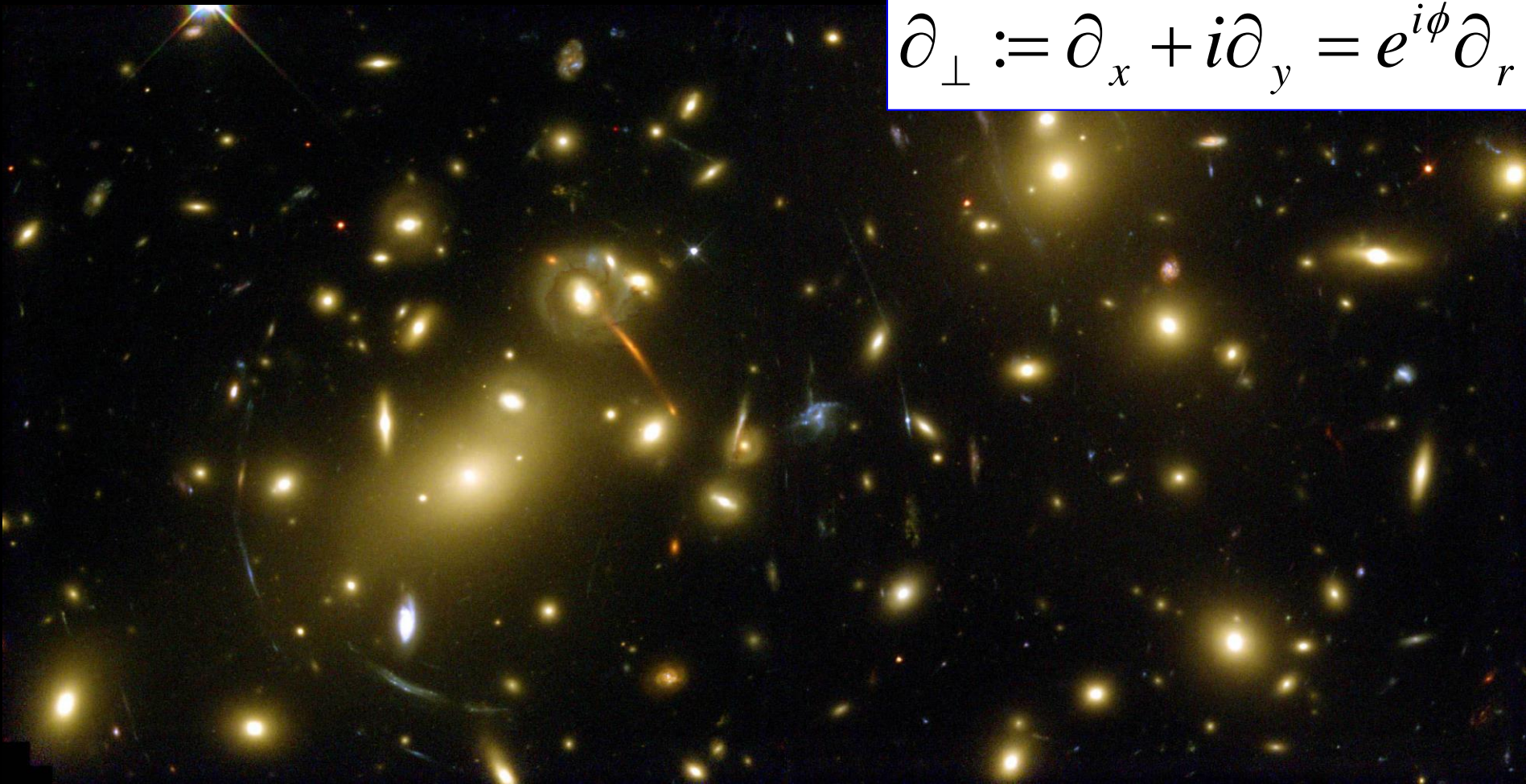
Weak field $|\Psi| \ll$ satisfied for extragalactic situations

$$\left| \frac{\Psi}{c^2} \right| \sim \frac{3}{2} \Omega_m \left(\frac{l_k}{r_H} \right)^2 \frac{\delta}{a}$$

Gravitational Shear

$$\gamma = \partial_{\perp} \partial_{\perp} \psi / 2$$

$$\partial_{\perp} := \partial_x + i\partial_y = e^{i\phi} \partial_r$$



Tangential Shear, γ_+

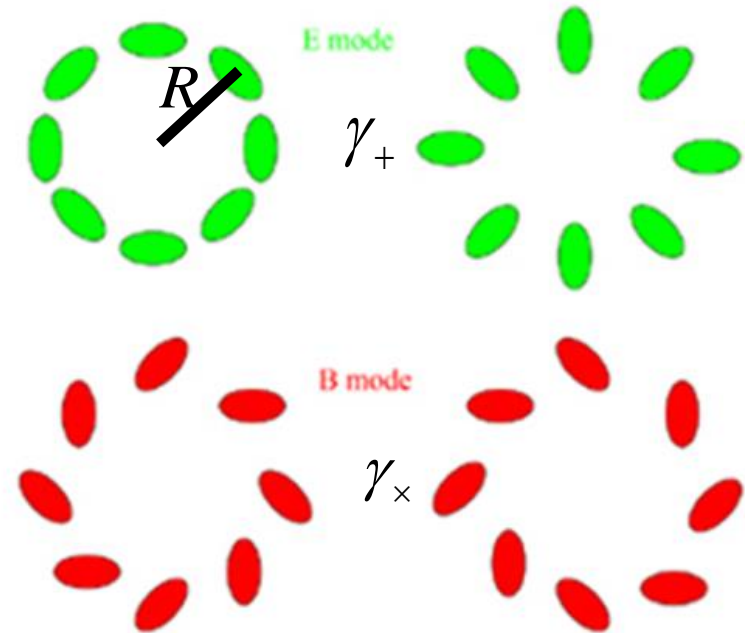
A measure of azimuthally-averaged tangential coherence of elliptical distortions around a given point (Kaiser 95):

$$\gamma_+(R) = \Delta\Sigma(R) / \Sigma_{\text{crit}}$$

$$(\Gamma_+)_{ij} = \left(\delta_i \delta_j - \frac{1}{2} \Delta^{(2)} \delta_{ij} \right) \psi_+$$

$$\gamma_\times(R) = 0$$

$$(\Gamma_\times)_{ij} = (\epsilon_{kj} \partial_i \partial_k - \epsilon_{ki} \partial_j \partial_k) \psi_\times$$



$\Delta\Sigma(R)$ is the *radially-modulated* surface mass density:

$$\Delta\Sigma(R) = \Sigma(< R) - \Sigma(R)$$

Sensitive to interior mass

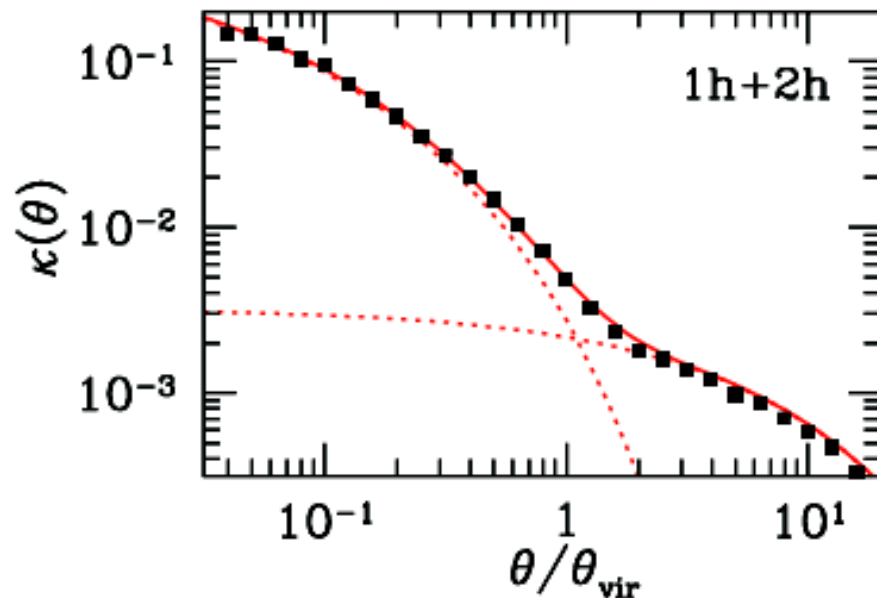
$$\Sigma(\mathbf{R}) = \int dl \delta\rho(\mathbf{R}, l)$$

Shear doesn't see mass sheet

Averaged lensing profiles in/around LCDM halos (Oguri+Hamana 11)

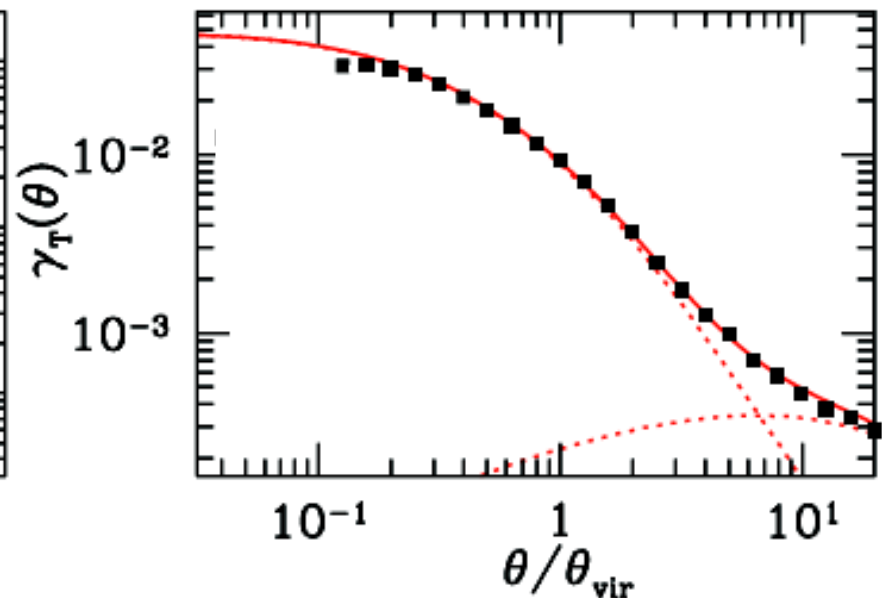
Total

$$\kappa = \Sigma(R) / \Sigma_{\text{crit}}$$



Modulated

$$\gamma_+ = \Delta\Sigma(R) / \Sigma_{\text{crit}}$$



- Tangential shear is a powerful probe of **1-halo term**, or **internal halo structure**.
- Shear alone cannot recover absolute mass, known as **mass-sheet degeneracy**:

γ remains unchanged by $\kappa \rightarrow \kappa + \text{const.}$

Gravitational Magnification

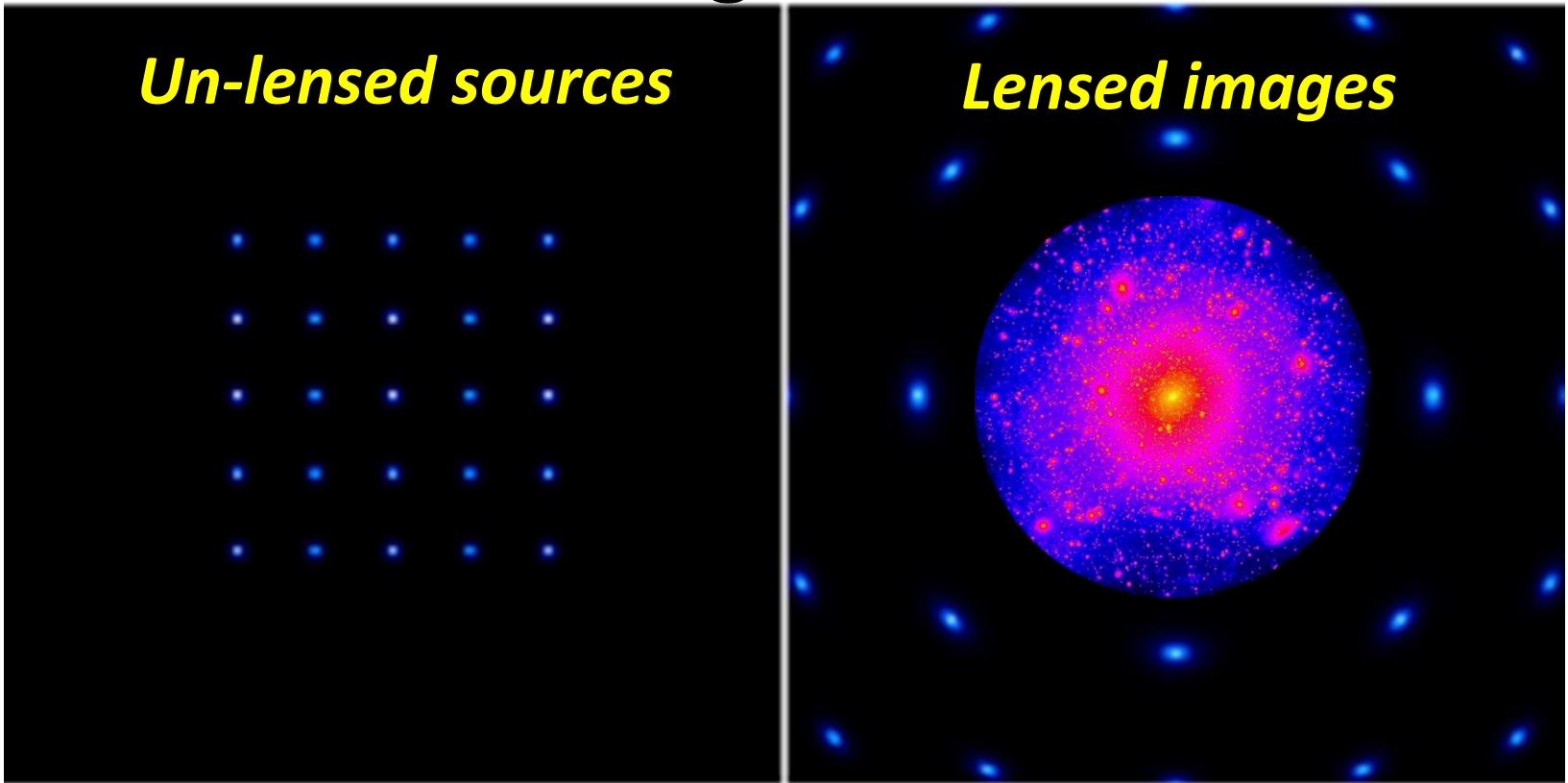
$$\kappa = \partial_{\perp} \partial_{\perp}^* \psi / 2 = \Delta_{\perp} \psi / 2$$

$$\partial_{\perp} := \partial_x + i\partial_y = e^{i\phi} \partial_r$$

MACSJ1149 (z=0.54)

Zheng+CLASH. 2012, *Nature*, 489, 406

Shear and Magnification Effects



Un-lensed sources

Lensed images

- **Shear**

Sensitive to “modulated” matter density

✓ Geometric shape dist: $\delta e_+ \sim \gamma_+$

$$\Sigma_{\text{crit}} \gamma_+ = \Delta \Sigma(R) \equiv \Sigma(< R) - \Sigma(R)$$

- **Magnification**

Sensitive to “total” matter density

✓ Flux amplification: μF
 ✓ Geometric area dist: $\mu \Delta \Omega$

$$\mu \approx 1 + 2\kappa; \quad \Sigma_{\text{crit}} \kappa = \Sigma(R)$$

Combining Shear and Magnification

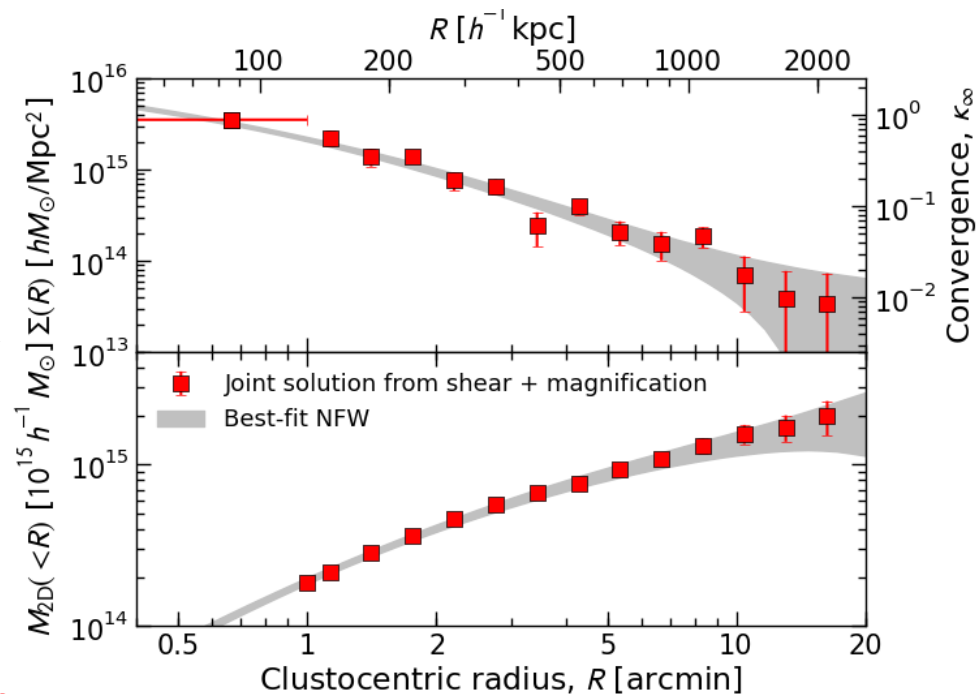
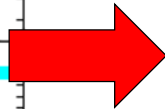
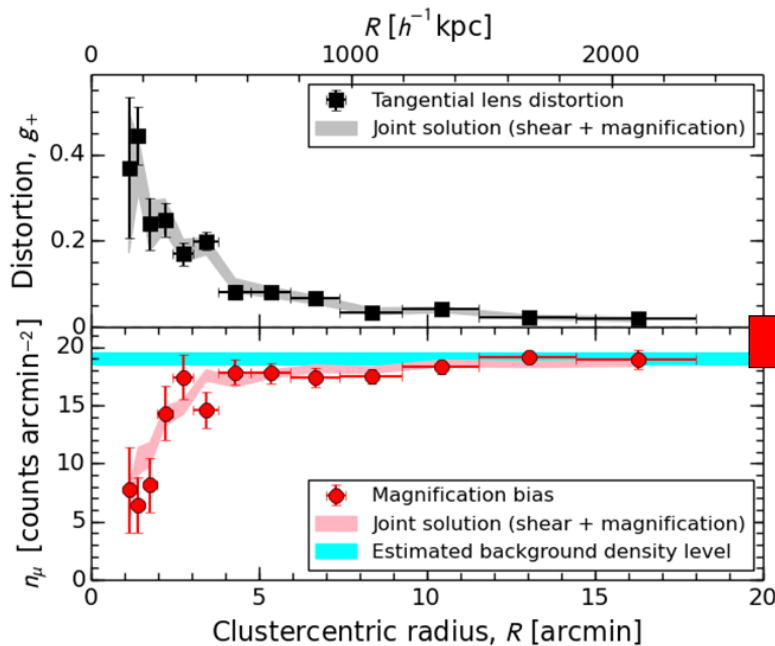
Bayesian joint-likelihood approach (Umetsu+11a, ApJ; Umetsu 13, ApJ)

Tangential distortion

$$g_+(R) = \frac{\kappa(< R) - \kappa(R)}{1 - \kappa(R)},$$

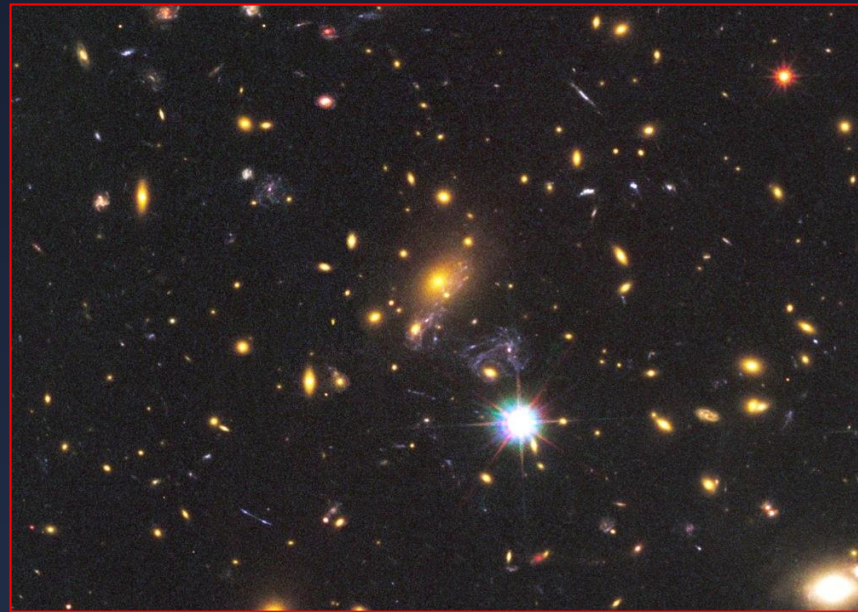
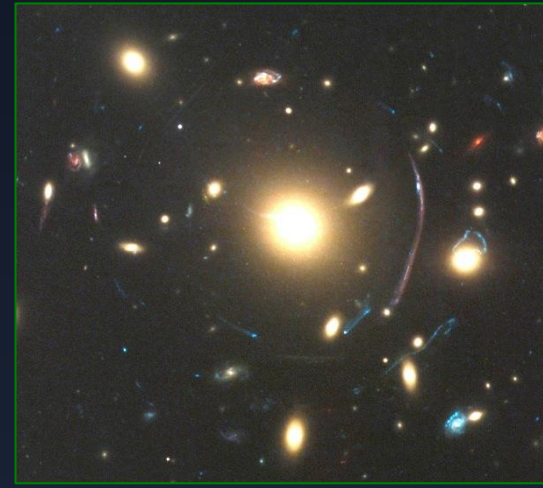
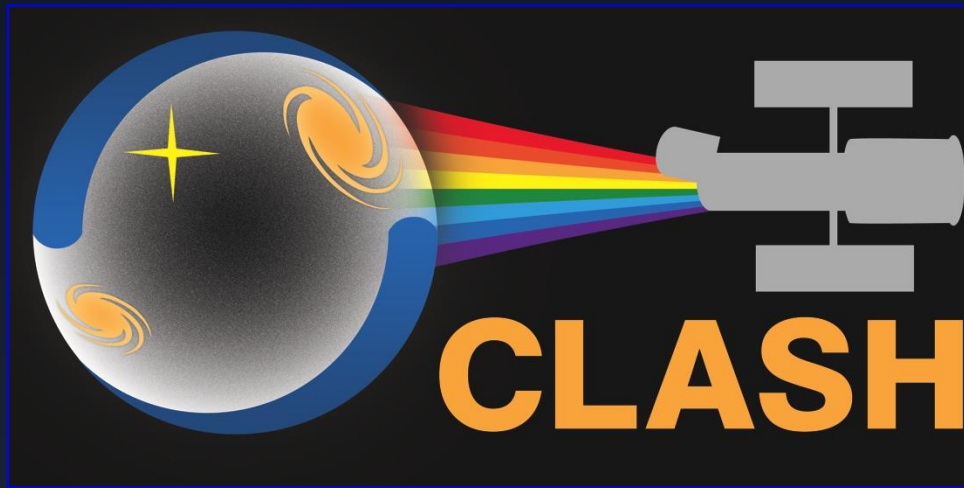
Magnification bias

$$\mu^{-1}(R) = [1 - \kappa(R)]^2 - [\kappa(< R) - \kappa(R)]^2$$



- Mass-sheet degeneracy broken
- Total statistical precision improved by $\sim 20\text{-}30\%$
- Calibration uncertainties marginalized over: $c = \{\langle W \rangle_s, f_{W,s}, \langle W \rangle_{\mu}, \bar{n}_{\mu}, s_{\text{eff}}\}$.

Cluster Lensing And Supernova survey with Hubble

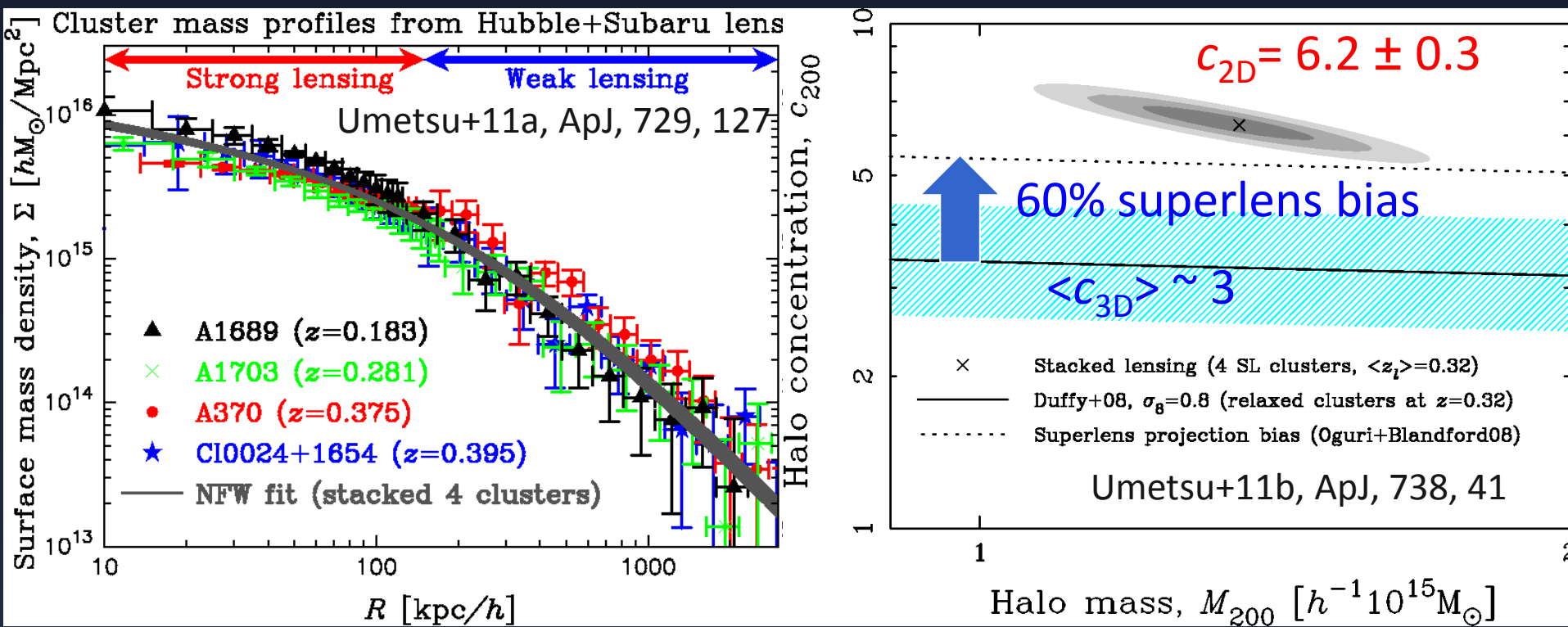


PI. Marc Postman (STScI)

<http://www.stsci.edu/~postman/CLASH/Home.html>

CLASH Objectives & Motivation

Before CLASH (2010), deep-multicolor Strong (*HST*) + Weak (Subaru) lensing data only available for a handful of “strong-lens” clusters



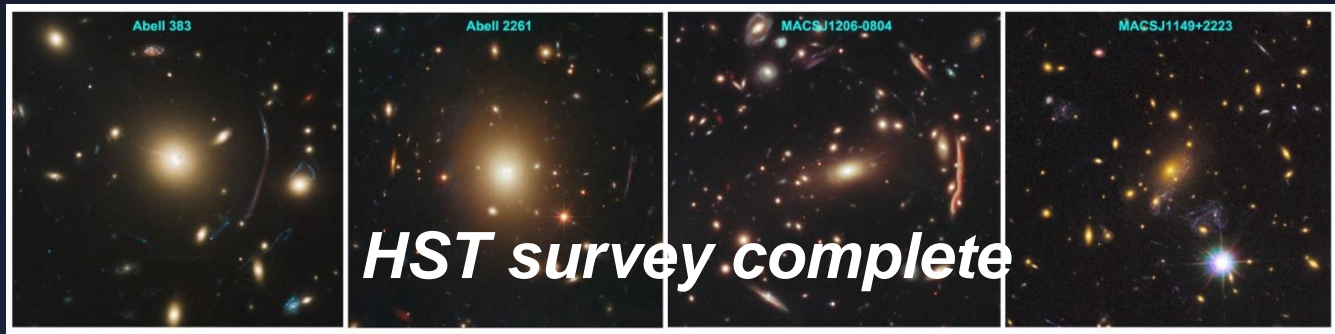
Total mass profile shape: consistent w CDM (self-similar universal profile)

Degree of concentration: maximum superlens correction not enough if $\langle c_{\text{LCDM}} \rangle \sim 3$?

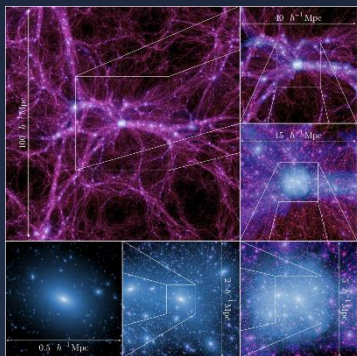


CLASH: Observational + Theory Efforts

A 524-orbit *HST* Treasury Program to observe 25 clusters in 16 filters ($0.23\text{-}1.6\ \mu\text{m}$) (Postman+CLASH 12)



Wide-field Subaru imaging ($0.4 - 0.9\ \mu\text{m}$) plays a unique role in complementing deep *HST* imaging of cluster cores (Umetsu+14, *ApJ*, arXiv:1404.1375)



MUSIC-2 (hydro + N-body re-simulation) provides an accurate characterization of CLASH sample with testable predictions (Meneghetti+14, arXiv:1404.1384)

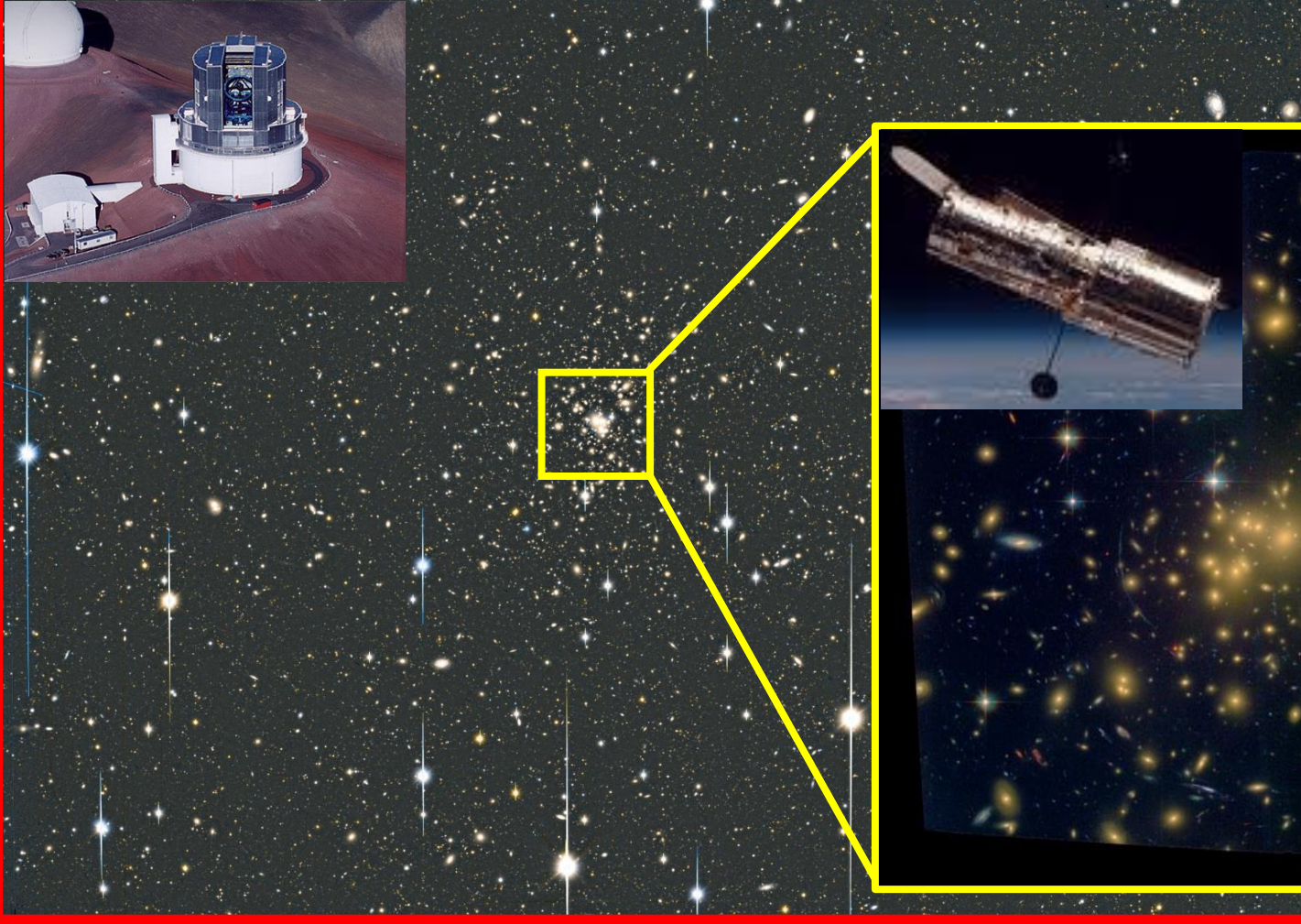
The CLASH Gallery (HST)



The final HST observation for CLASH was on 9-July-2013 ... 963 days, 15 hrs, 31 min after first obs.

***SUBARU* multi-color imaging for wide-field weak lensing**

High-resolution space imaging with *Hubble* for strong lensing





CLASH: Sample Definition

- Redshift coverage
 - $0.18 < z < 0.90$
- X-ray morphology + T_x selection
 - $T_x > 5\text{keV}$
 - Small BCG to X-ray-peak offset, $\sigma_{\text{off}} \sim 10\text{kpc}/h$
 - Smooth regular X-ray morphology
- **Optimized for radial-profile analysis ($R > 2 \sigma_{\text{off}} \sim 20\text{kpc}/h$)**
- CLASH theoretical predictions (Meneghetti+CLASH 14)
 - Composite relaxed (70%) and unrelaxed (30%) clusters
 - Mean $\langle c_{200c} \rangle = 3.9$, $\sigma(c_{200c}) = 0.6$, $c_{200c} = [3, 6]$
 - >90% of CLASH clusters to have strong-lensing features



CLASH-WL Results [1]

Ensemble-averaged internal halo structure:

- Halo mass density profile, $\langle \Delta \Sigma(R) \rangle$
- Degree of mass concentration, $\langle c_{200} \rangle$

from *stacked WL-shear-only* analysis of CLASH clusters

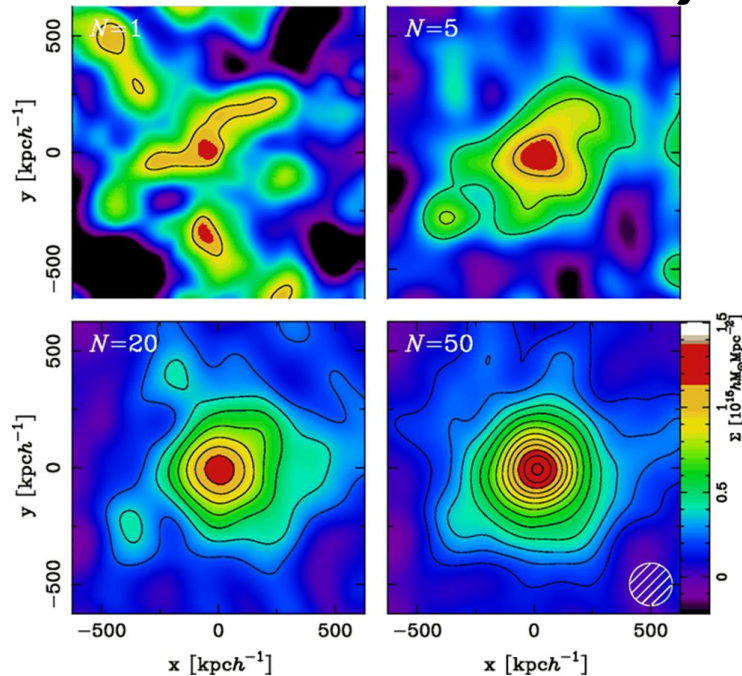


Figure from Okabe, Smith, Umetsu+14, ApJL, 769, 35

Ensemble-averaged DM halo profile

Stacking of weak-lensing signals by weighting individual clusters according to the sensitivity kernel matrix:

$$\langle\langle \widehat{\Delta\Sigma}_+ \rangle\rangle = \left(\sum_n \mathcal{W}_{+n} \right)^{-1} \left(\sum_n \mathcal{W}_{+n} \widehat{\Delta\Sigma}_{+n} \right),$$

with the individual sensitivity matrix

$$(\mathcal{W}_{+n})_{ij} \equiv \Sigma_{c,n}^{-2} (C_{+n}^{-1})_{ij}$$

defined with the total covariance matrix

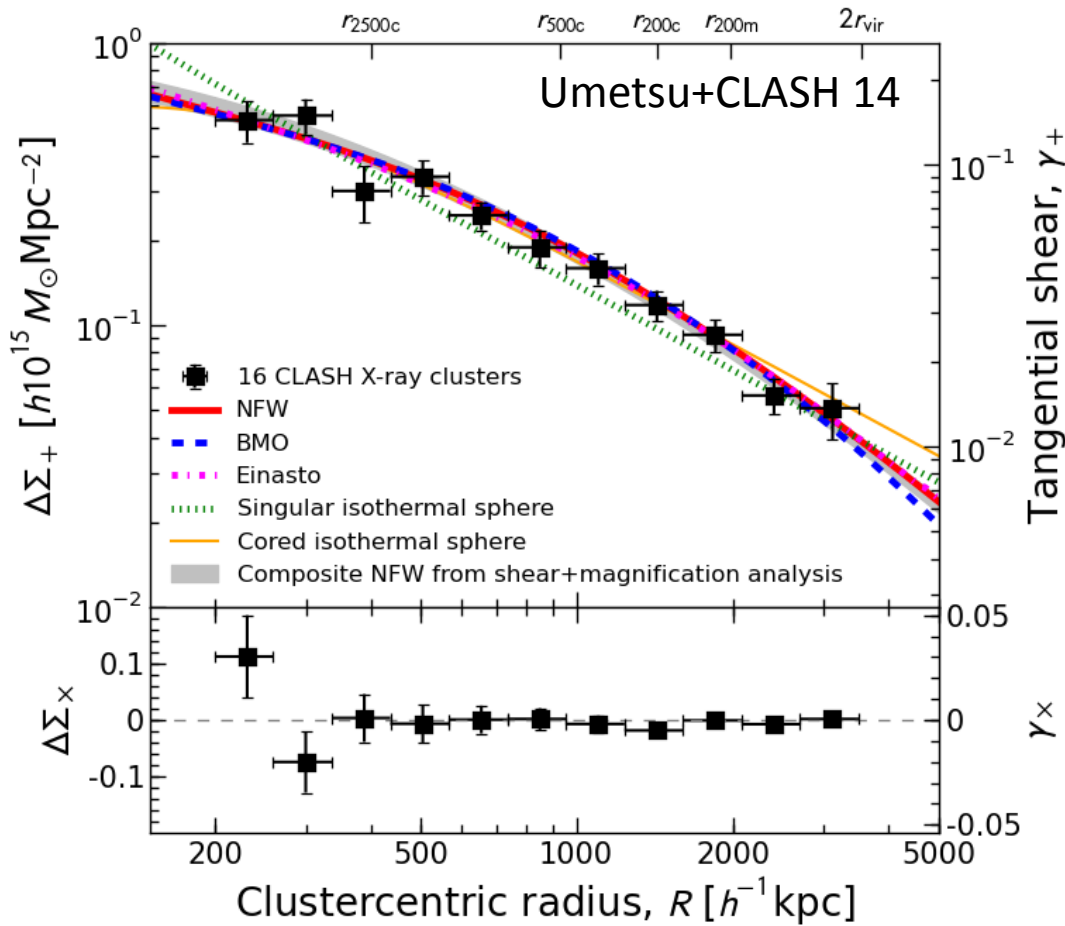
$$C_+ = C_+^{\text{stat}} + C_+^{\text{sys}} + C_+^{\text{lss}}.$$

With “trace-approximation”, averaging is interpreted as

$$\langle\langle \Sigma_c^{-1} \rangle\rangle = \frac{\sum_n \text{tr}(\mathcal{W}_{+n}) \Sigma_{c,n}^{-1}}{\sum_n \text{tr}(\mathcal{W}_{+n})},$$



Stacked halo density profile $\Delta\Sigma(R)$



Stacked shear-only analysis provides a net 1-halo-only constraint ($\gamma_{+,2h} < 1e-3$)

NFW an excellent fit (PTE = 0.66)

- $M_{200c} = (1.3 \pm 0.1) 10^{15} M_{\text{sun}}$
 - $c_{200c} = 4.01 (+0.35, -0.32)$
- at $\langle z \rangle = 0.35$

Corresponding to $\theta_{\text{Ein}} = (15'' \pm 4'')$ at $z_s = 2$, consistent w SL analysis, $\langle \theta_{\text{Ein}} \rangle \sim 20''$ (Zitrin+14, in prep)

Consistent w a family of density profiles for collisionless DM halos (NFW, variants of NFW, Einasto)

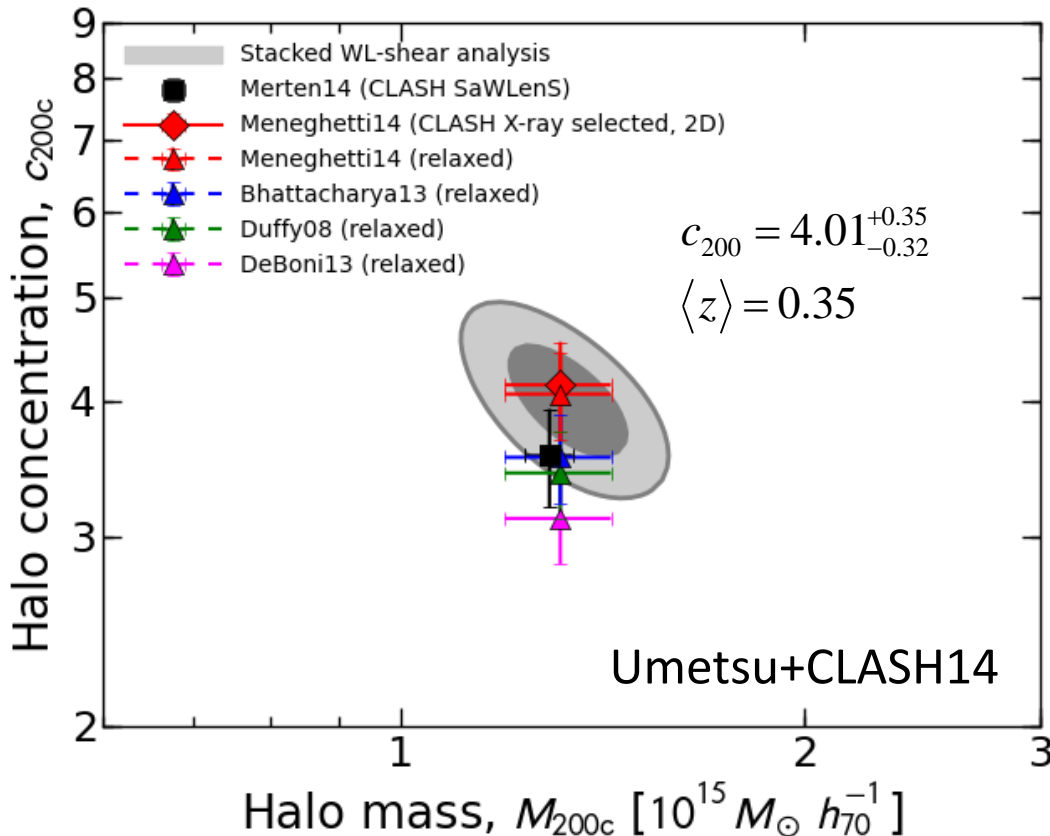


Integrated constraints on $c(M_{200c}, z)$

Theoretical predictions

for stacked $c(M, z)$

$$\langle c_{200c} \rangle = \frac{\int dM dz N(M, z) \hat{c}_{200c}(M, z)}{\int dM dz N(M, z)} \approx \frac{\sum_n \text{tr}(\mathcal{W}_n) \hat{c}_{200c}(M_n, z_n)}{\sum_n \text{tr}(\mathcal{W}_n)}$$



Variance in theory due to different cosmology (σ_8) and mass resolution

M14 (CLASH, WMAP7): $\sigma_8 = 0.82$

Bhat13: $\sigma_8 = 0.8$

Duffy08: $\sigma_8 = 0.8$

DeBoni13: $\sigma_8 = 0.78$

- Excellent agreement w CLASH predictions (M14), $c_{200c} \sim 4$
- Consistent w Bhatt13, Duffy08 predictions at 1σ , $c_{200c} \sim 3.6$



CLASH-WL Results [2]

Reconstruction of **individual cluster structures**:

- Projected mass density profiles $\Sigma(R)$
- Deprojected spherical mass estimates $M(<r)$

from **joint shear+magnification analysis** of CLASH clusters



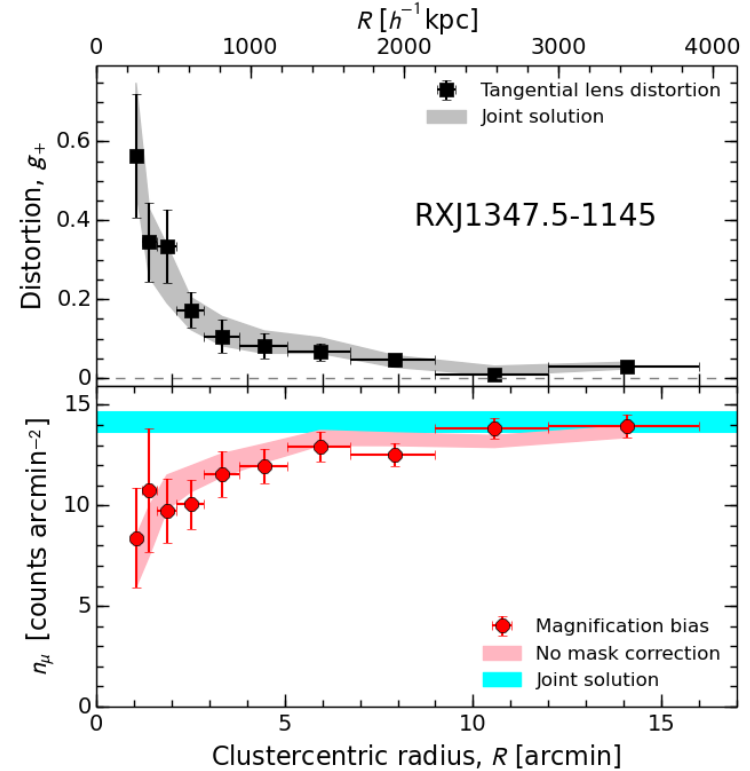
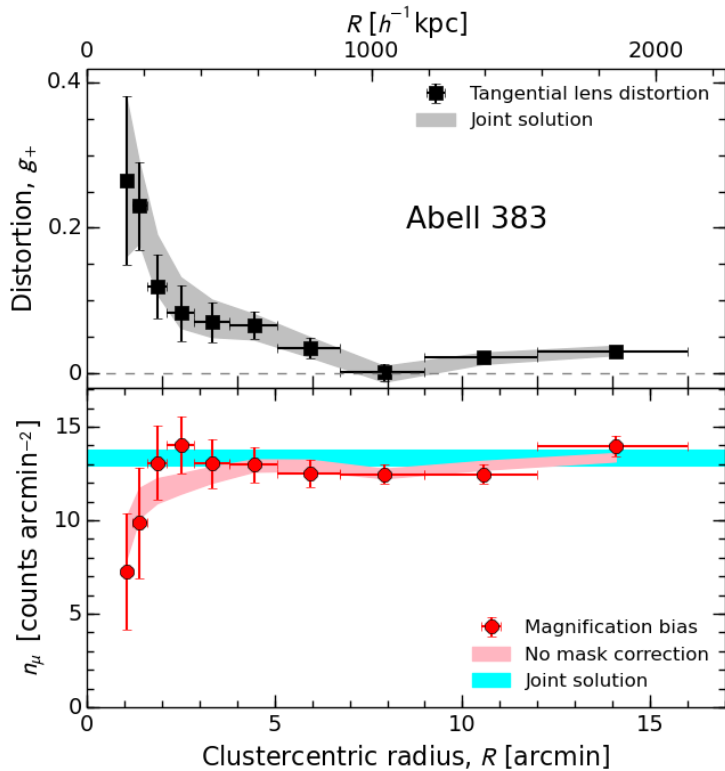
CLASH-WL: Joint Shear + Magnification Analysis

CLASH low mass

$M_{200c} = 6e14 M_{\text{sun}}/h$ ($z=0.19$)

CLASH high mass

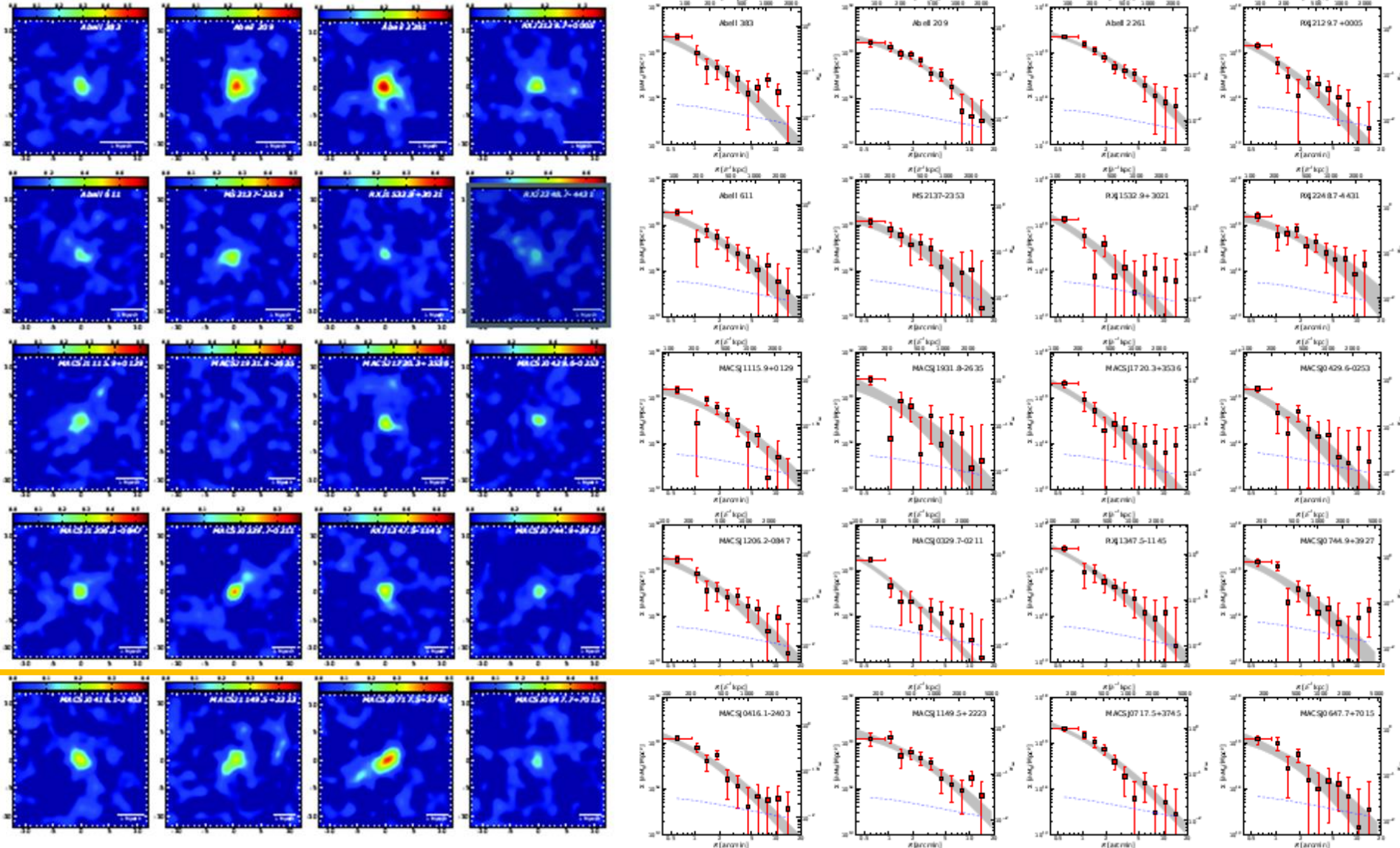
$M_{200c} = 20e14 M_{\text{sun}}/h$ ($z=0.45$)



Shear-magnification consistency: $\langle \chi^2/\text{dof} \rangle = 0.92$ for 20 CLASH clusters



Mass Density Profile Dataset

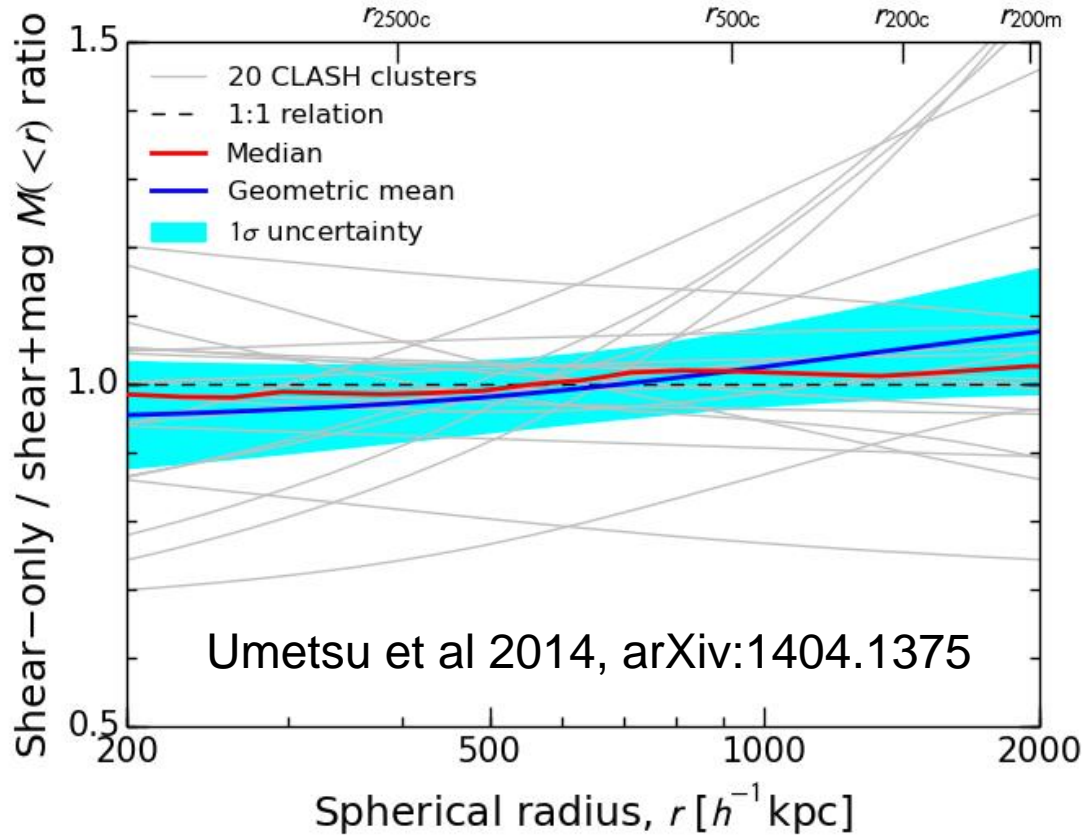


Umetsu et al. 2014, ApJ, accepted (arXiv:1404.1375)



Shear-Magnification Consistency

$M(<r)$ de-projected assuming spherical NFW (20 CLASH clusters)

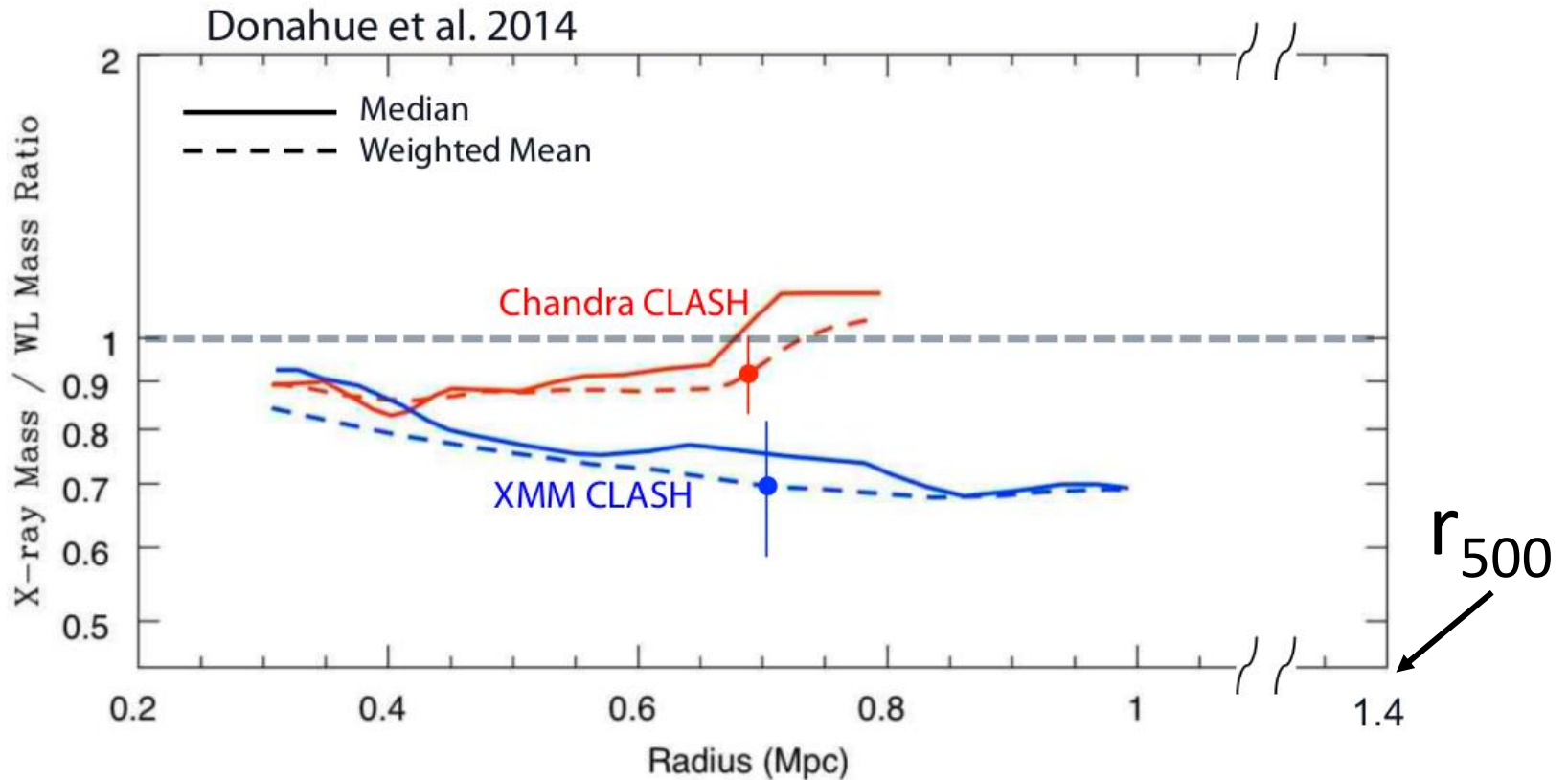


Umetsu et al. 14,
ApJ, accepted
(arXiv:1404.1375)

Internal systematic uncertainty in the overall mass calibration,
empirically derived to be about +/- 8%



CLASH: WL vs. X-ray Mass Comparison



X-ray to WL mass comparison at r_{500}

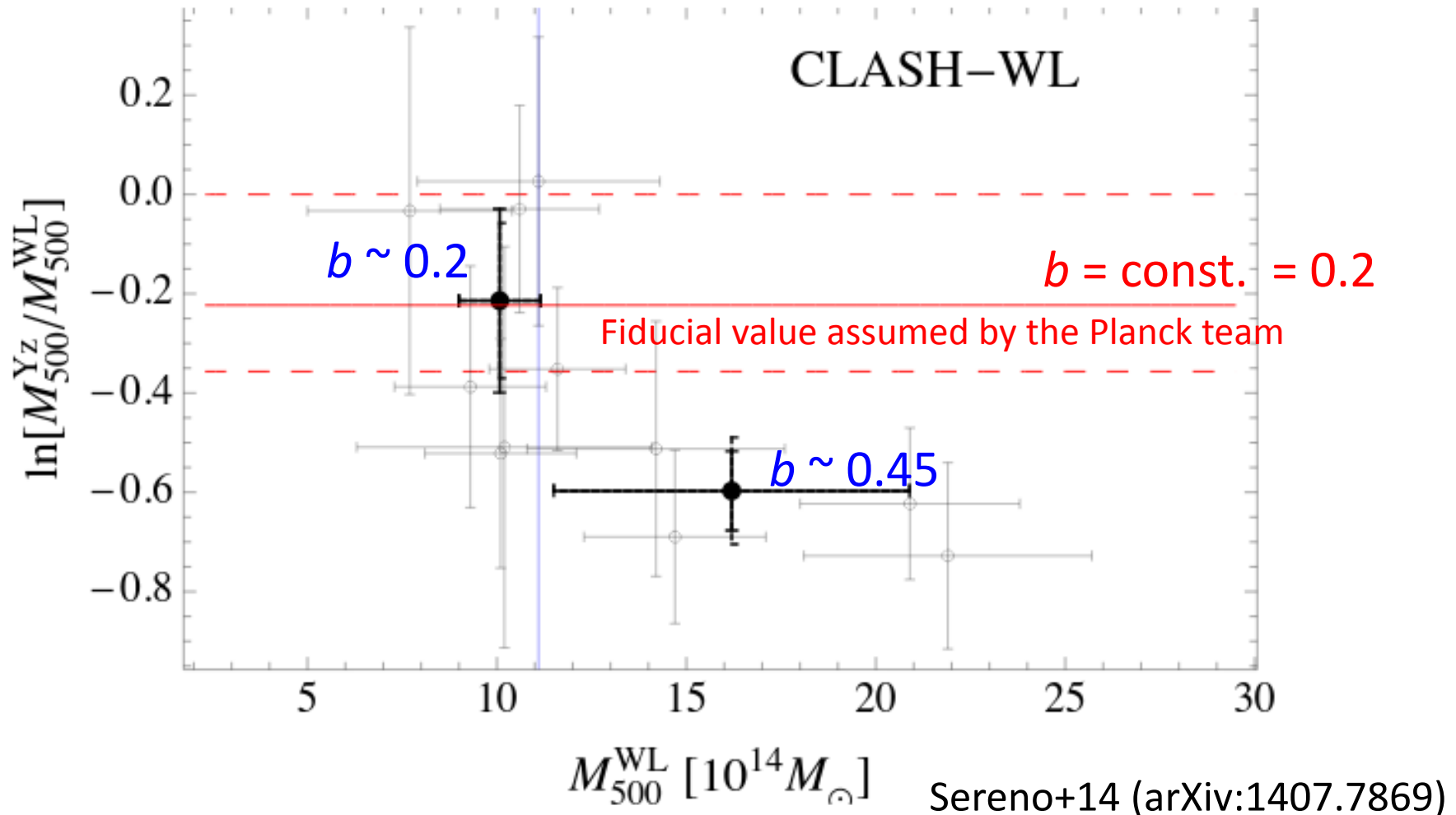
- $b = 1 - \langle M_{\text{Chandra}} / M_{\text{WL}} \rangle = 0.22 \pm 0.10$
- $b = 1 - \langle M_{\text{XMM}} / M_{\text{WL}} \rangle = 0.44 \pm 0.06$

Donahue+CLASH
14, ApJ, accepted
(arXiv:1405.7876)



Comparison with *Planck* Masses

Mass-dependent bias (20-45%) observed for *Planck* mass estimates





Shear + Magnification + Strong Lensing

Ensemble-averaged total mass density profile

$$\langle \Sigma(R) \rangle = \Sigma_{1h}(R) + \Sigma_{2h}(R)$$

around the CLASH cluster sample

Clustering of matter
around halos with M :

$$\xi_{\text{hm}}(r | M) = \frac{\langle \rho_{1h}(r | M) \rangle}{\bar{\rho}} + b_h(M) \xi_{\text{mm}}(r)$$

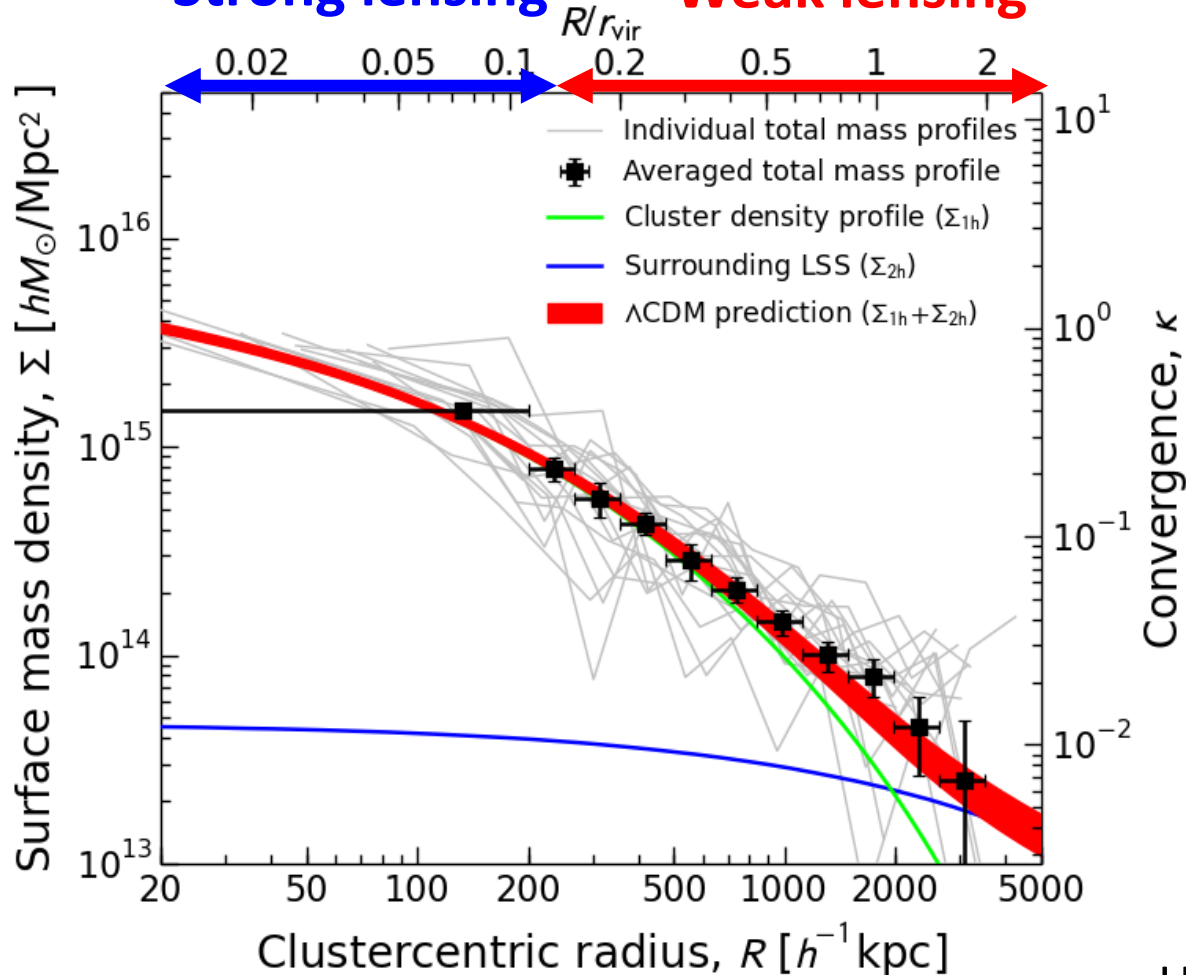
1h term

2h term



Averaged cluster (1h) + LSS (2h) from WL shear + magnification + SL

Strong lensing **Weak lensing**



Adding Strong Lensing (SL) tightly constrains the inner density profile ($R < 100 \text{ kpc}/h$)

Inner mass profiles from SL follow 1h prediction from outer WL-shear information

Recovered mass-sheet (LSS), consistent w the shear-based halo model prediction, $b_h = 9$ (WMAP7+Tinker10)

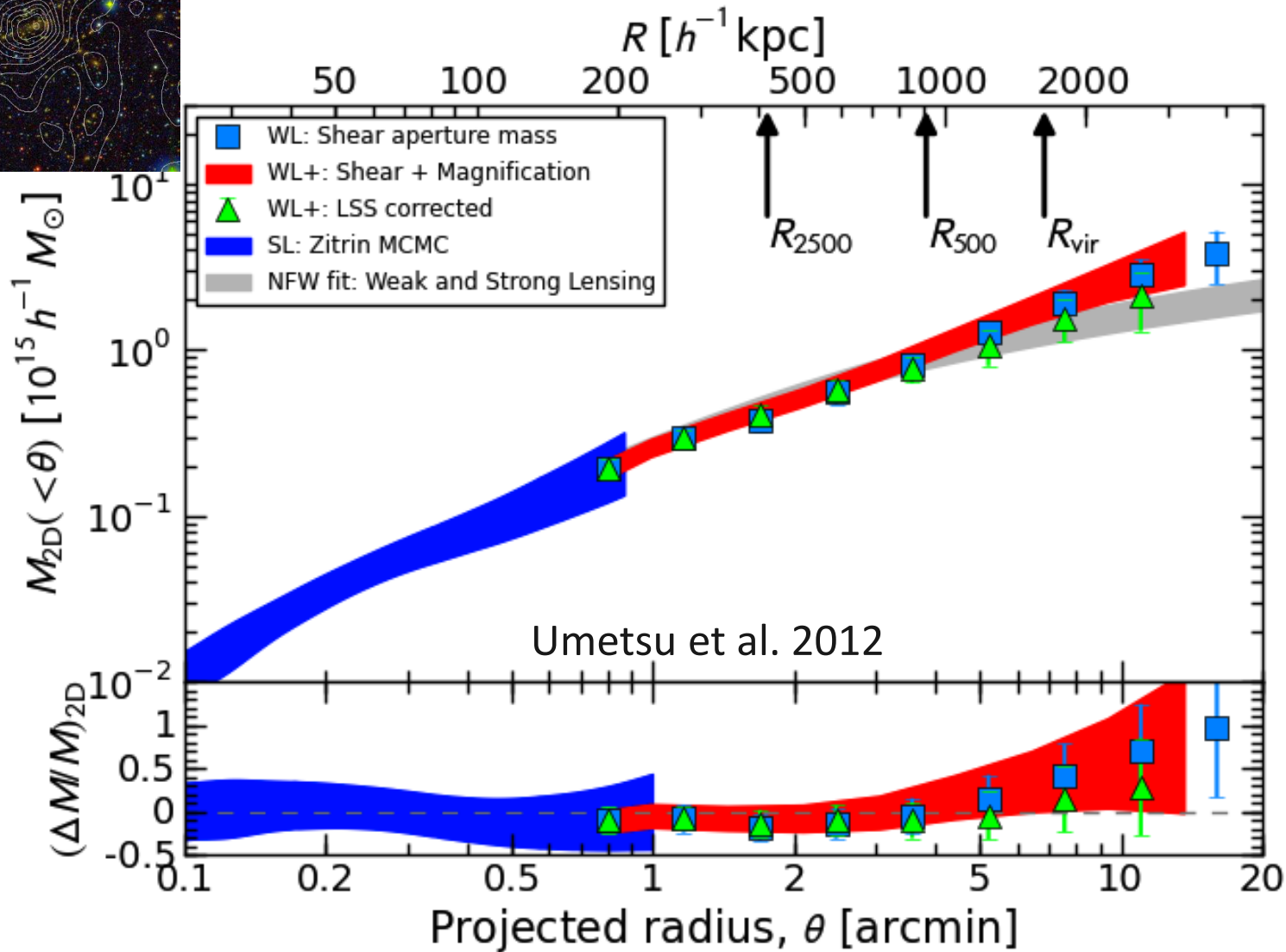
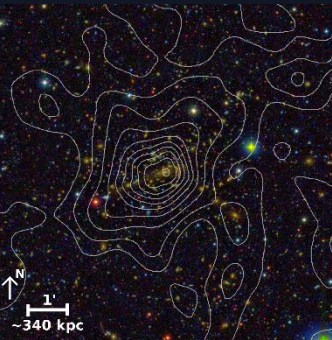
Constraints on the Intracluster Dark-Matter Equation of State

A Case study from the ongoing CLASH-VLT
redshift survey

MACS1206 ($z=0.44$): A relaxed CLASH cluster



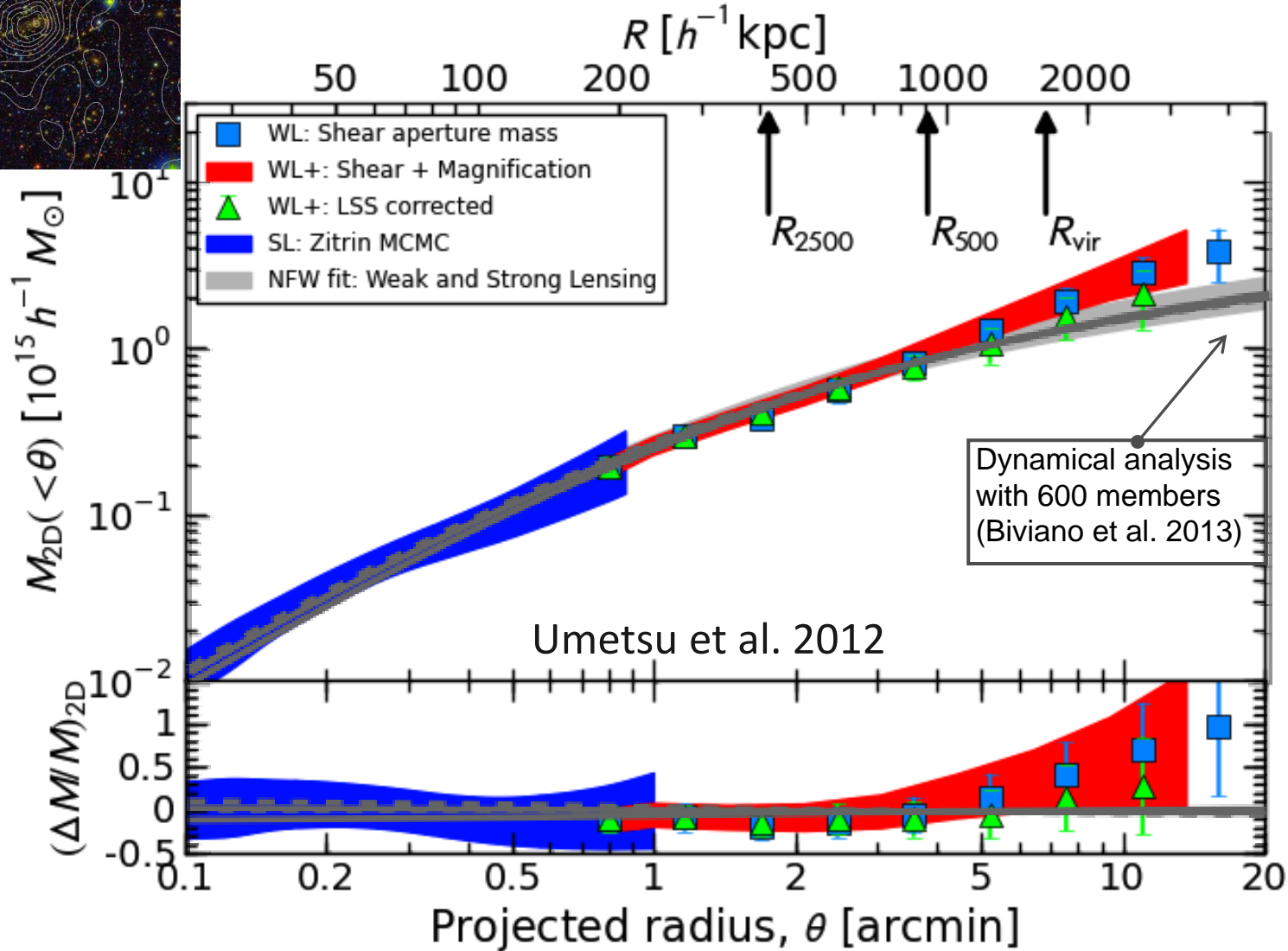
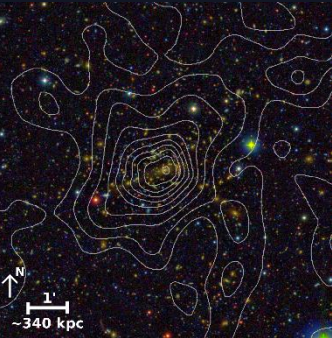
Total mass profiles from completely independent methods agree.



MACS1206 (z=0.44): A relaxed CLASH cluster



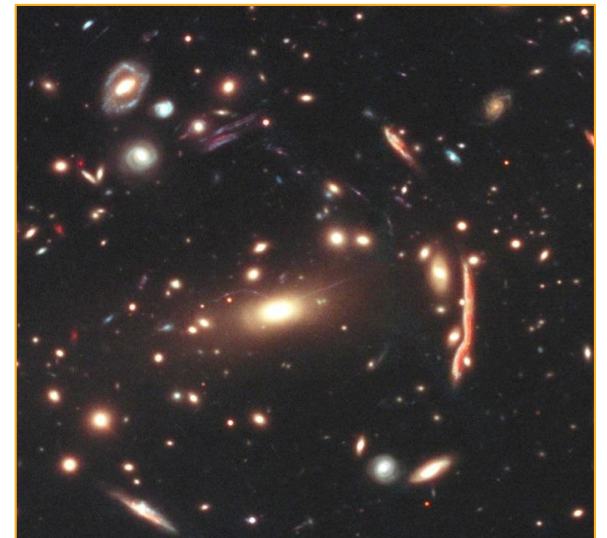
Total mass profiles from completely independent methods agree.



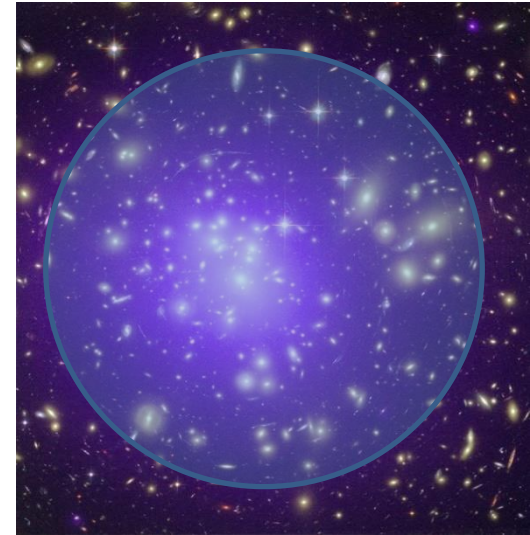
Constraining DM Equation of State

- By testing whether intracluster DM is pressureless ($w=0$) using cluster mass profiles $M(<r)$ of MACS1206 determined from 2-independent ways:
 - **Gravitational lensing with HST+Subaru** (Umetsu+2012)
 - **Galaxy kinematics with VLT/VIMOS** (Biviano+2013)
- Test made possible by our high-quality CLASH data for an equilibrium cluster:

$$w(r) = \frac{p_r(r) + 2p_t(r)}{c^2 3\rho(r)}$$



Framework



Consider the static, spherically-symmetric metric within a DM halo of the form:

$$ds^2 = -e^{-2\Phi(r)} dt^2 + \left[1 - \frac{2Gm(r)}{r}\right]^{-1} dr^2 + r^2 d\Omega^2.$$

Consider an intracluster DM fluid with anisotropic pressure. In this metric, the Einstein field equations read:

$$\begin{aligned}\rho(r) &= \frac{1}{8\pi G} \frac{m'}{r^2}, \\ p_r(r) &= -\frac{1}{8\pi G} \frac{2}{r^2} \left[\frac{m}{r} - r\Phi' \left(1 - \frac{2m}{r}\right) \right], \\ p_t(r) &= \frac{1}{8\pi G} \left\{ \left(1 - \frac{2m}{r}\right) \left[\frac{\Phi'}{r} + \Phi'^2 + \Phi'' \right] - \left(\frac{m}{r}\right)' \left(\frac{1}{r} + \Phi'\right) \right\}.\end{aligned}$$

The equation of state of this DM fluid is defined as

$$w(r) = \frac{p_r + 2p_t}{3\rho}.$$

Consider the weak-field limit, $|\Phi| \ll 1$, $Gm/r \ll 1$.

DM EoS from Kinematics+Lensing

The Jeans equation provides a way to measure the cluster mass profile from **cluster galaxy kinematics**

$$m_K(r) = -\frac{r\sigma_r^2}{G} \left[\frac{d \ln n_g}{d \ln r} + \frac{d \ln \sigma_r^2}{d \ln r} + 2\beta \right],$$

where galaxies as the probe particles are non-relativistic, $\sigma_r, \sigma_t \ll 1$ with $\beta = 1 - \sigma_t^2/(2\sigma_r^2)$. In our metric, the kinematic mass profile is related to the potential by

$$m_K(r) = \frac{r^2}{G} \Phi' \approx 4\pi \int [1 + 3w(r)] r^2 \rho(r) dr.$$

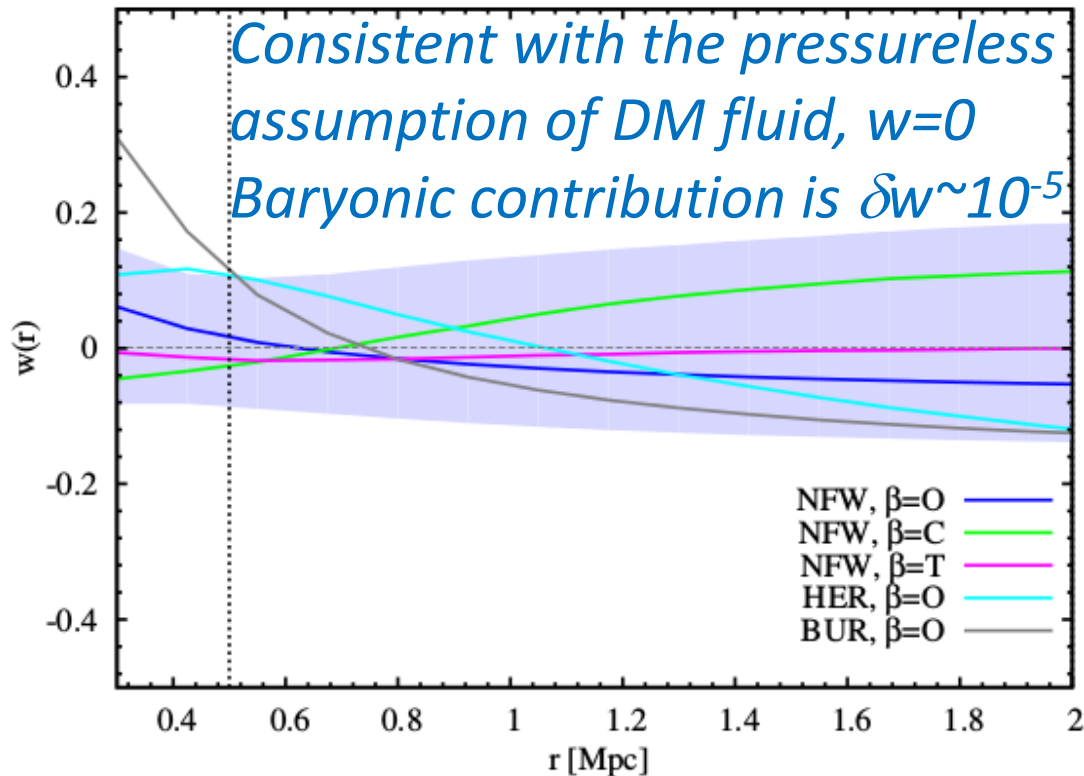
Gravitational lensing is sensitive to g_{00} and g_{rr} . Hence, its potential and associated mass profile are defined by

$$2\Phi_l \equiv \Phi + G \int \frac{m(r)}{r^2} dr,$$
$$m_L(r) \equiv \frac{r^2}{G} \Phi'_l = \frac{1}{2} [m_K(r) + m(r)].$$

To first order, the DM equation of state is sensitive to the derivatives of the lensing and kinematic mass profiles:

$$w(r) \approx \frac{2 m'_K(r) - m'_L(r)}{3 m'_L(r) - m'_K(r)}.$$

First application to a relaxed cluster



$$\langle w \rangle = 0.00 \pm 0.15(stat) + 0.08(syst)$$

In CLASH, we have 11 more clusters with VLT redshift measurements to improve the DM EoS constraint



Summary

- Ensemble-averaged halo structure $\Delta\Sigma$ (1h) of CLASH clusters is consistent with a family of standard collisionless CDM predictions:
 - $M_{200c} = (1.3 \pm 0.1) 10^{15} M_{\text{sun}}, \langle z \rangle = 0.35$
 - $c_{200c} = 4.01 (+0.35, -0.32)$
- Stacked-mean concentration agrees with:
 - theoretical expectation (WMAP7: $\Omega_m = 0.27, \Omega_\Lambda = 0.73, \sigma_8 = 0.82$), $\langle c_{200c} \rangle \sim 3.9$, which accounts for CLASH selection function and projection effects
 - measured effective Einstein radius, $\langle \theta_{\text{Ein}} \rangle = 20''$ ($z_s = 2$), from independent HST-SL analysis (Zitrin+CLASH 14, in prep)
- Previous overconcentration problems can be explained by
 - Theoretical predictions were likely underestimated (10-20%) in the high-mass cluster regime, $M_{200c} > 5e14 M_{\text{sun}}/h$ (e.g., σ_8)
 - Orientation bias due to halo triaxiality, boosting $\Sigma(R)$ at $R < 500 \text{kpc}/h$, resulting in $\sim +50\%$ bias in c_{200c} (Oguri+12)

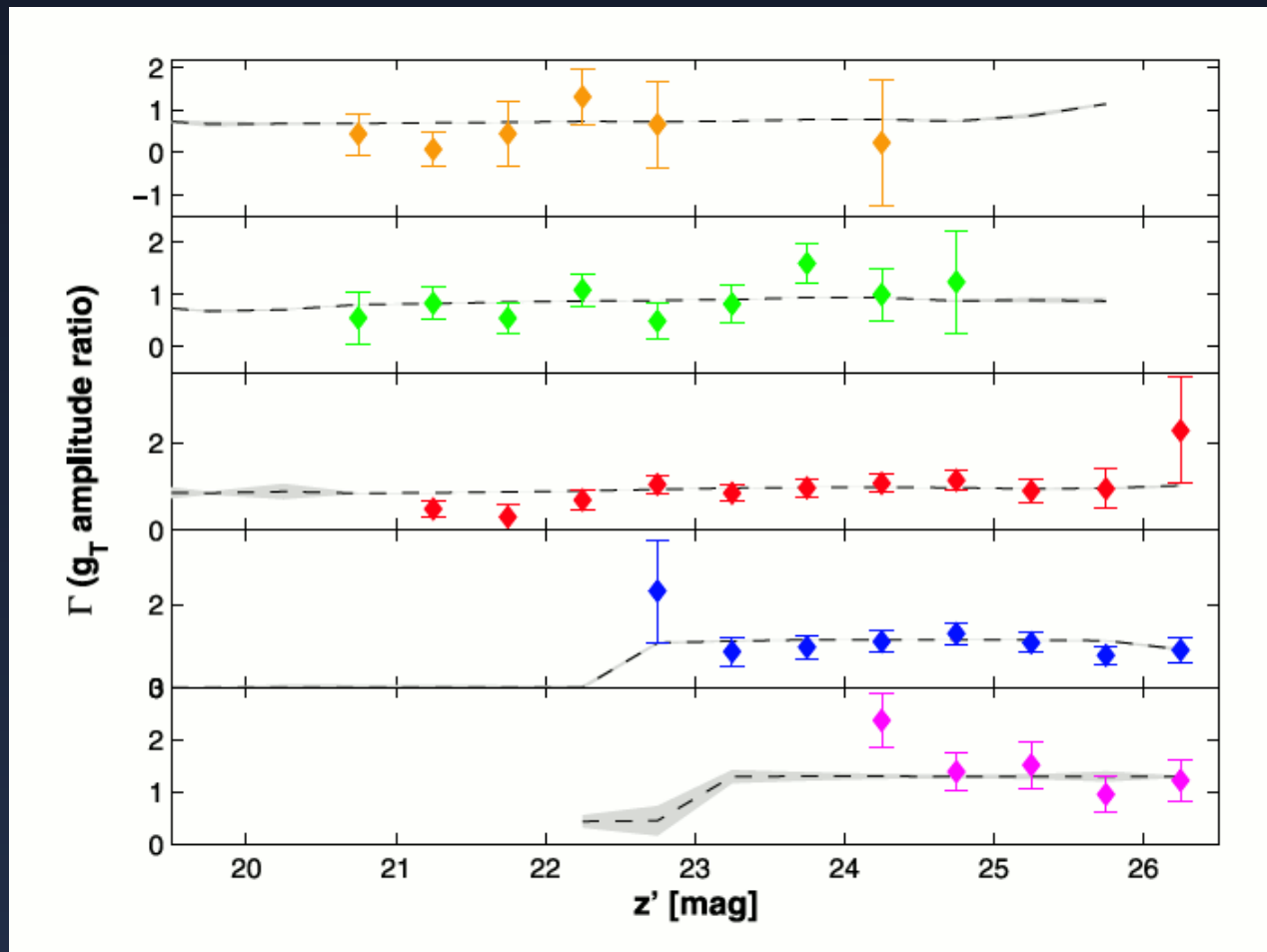


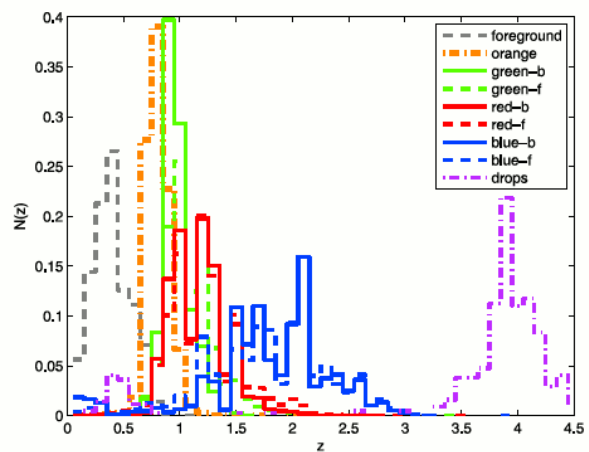
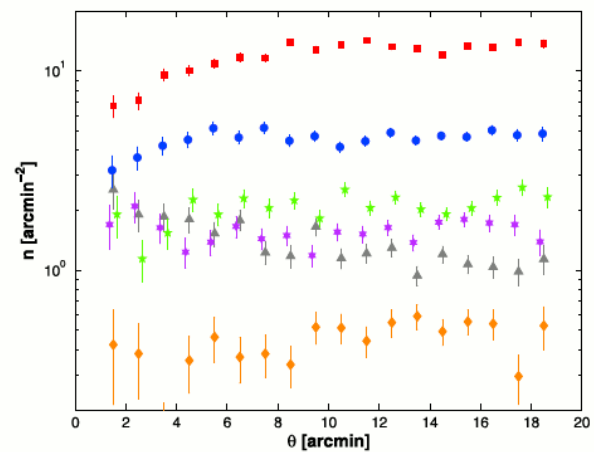
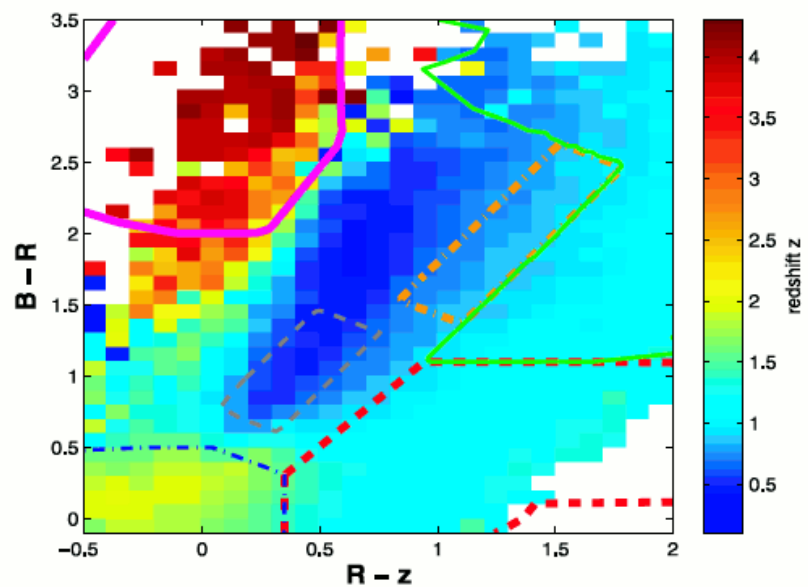
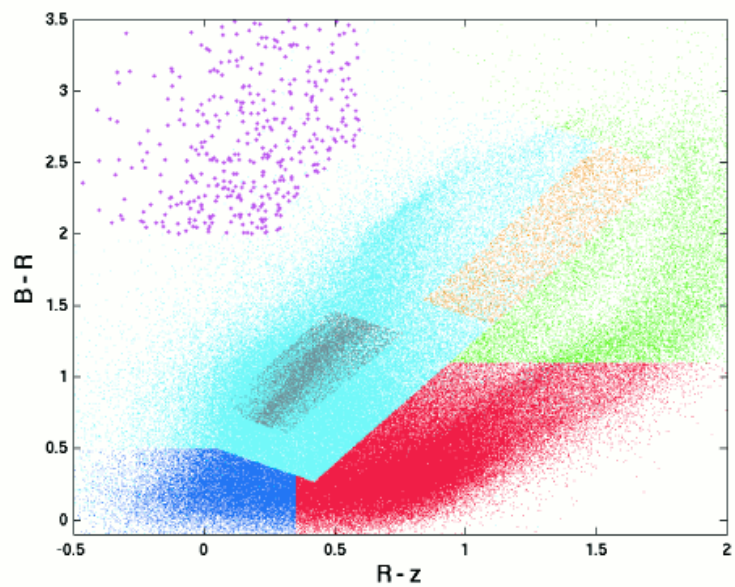
Summary (contd.)

- Consistent shear vs. magnification measurements allow for accurate cluster mass profile measurements for 20 CLASH clusters with $\pm 8\%$ systematic mass-calibration uncertainty.
- Averaged total matter distribution $\langle \Sigma \rangle$ (1h+2h) from full-lensing analysis (SL + shear + magnification) is consistent with shear-based halo model predictions ($b_h=9$ at $M_{200c}=1.3e15M_{sun}$, $z=0.35$), establishing further consistency in the context of LCDM.
- Our lensing+kinematics study of a single cluster found the DM EoS to be $\langle w \rangle = 0.00 \pm 0.15 \pm 0.08$ within $R=0.5-2\text{Mpc}$, confirming the standard pressureless assumption of DM fluid. A full CLASH-VLT sample of 12 clusters will further tighten the constraint on DM EoS.

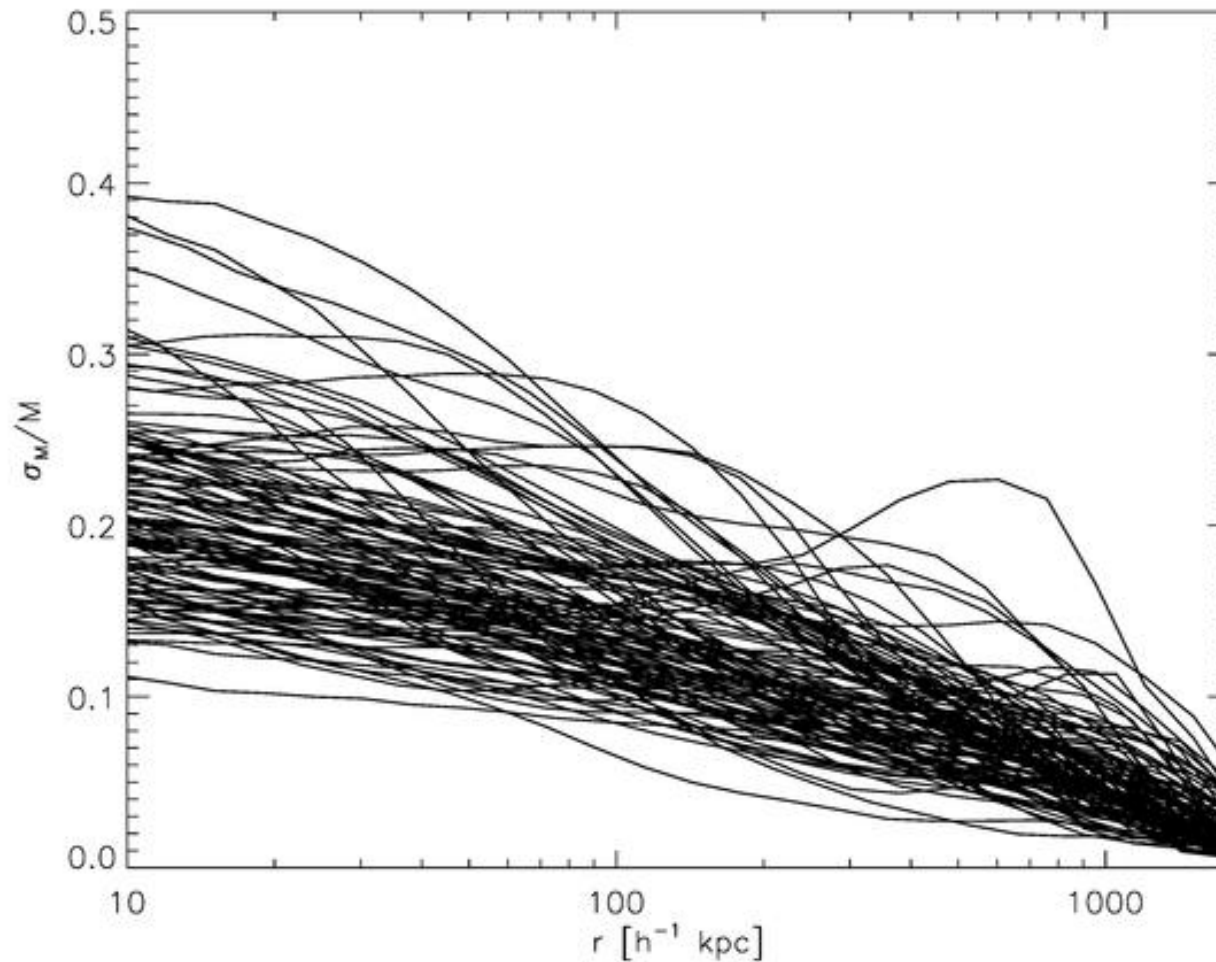
Supplemental Slides

SUBARU shear strength as a function of magnitude



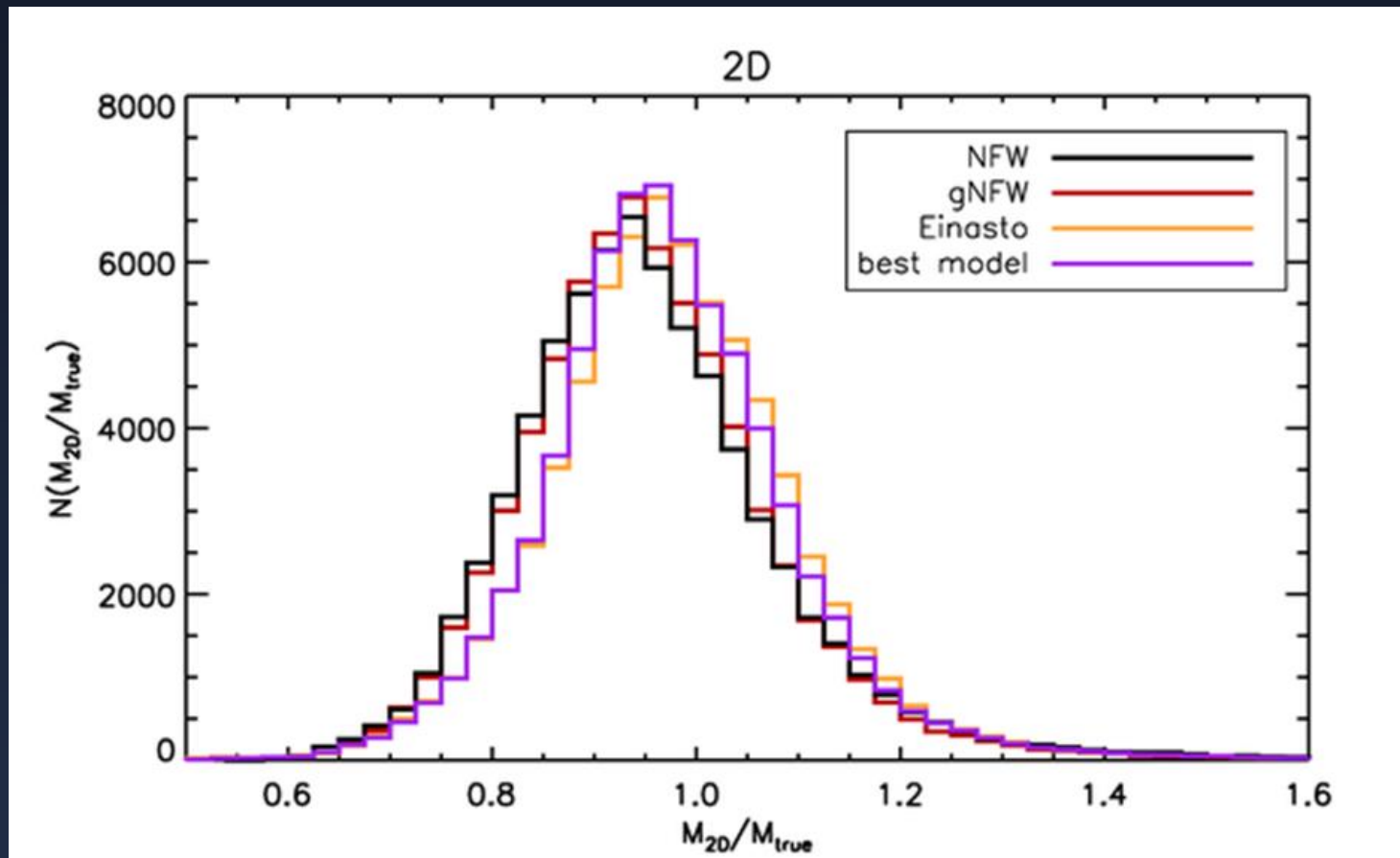


Scatter in $M_{2D}(R)$ by halo triaxiality



MUSIC-2 simulation by Massimo

Cluster masses recovered from lensing analysis

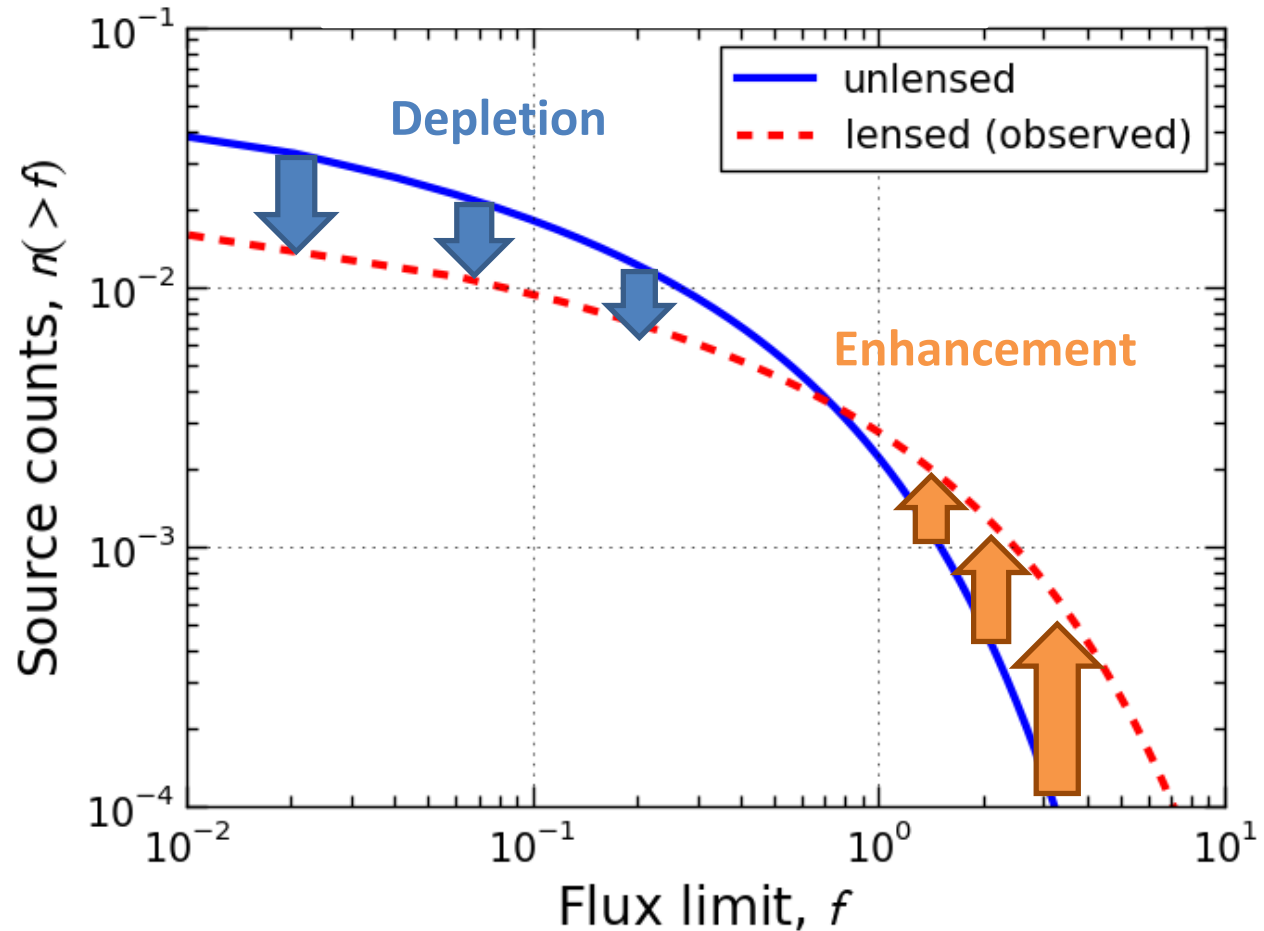


Magnification bias effects

Flux-limited
source counts:

$$n_{\text{obs}}(> f) = \mu^{-1} n(> \mu^{-1} f)$$

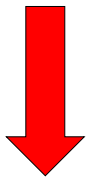
Broadhurst, Taylor &
Peacock 95



Flux amplification



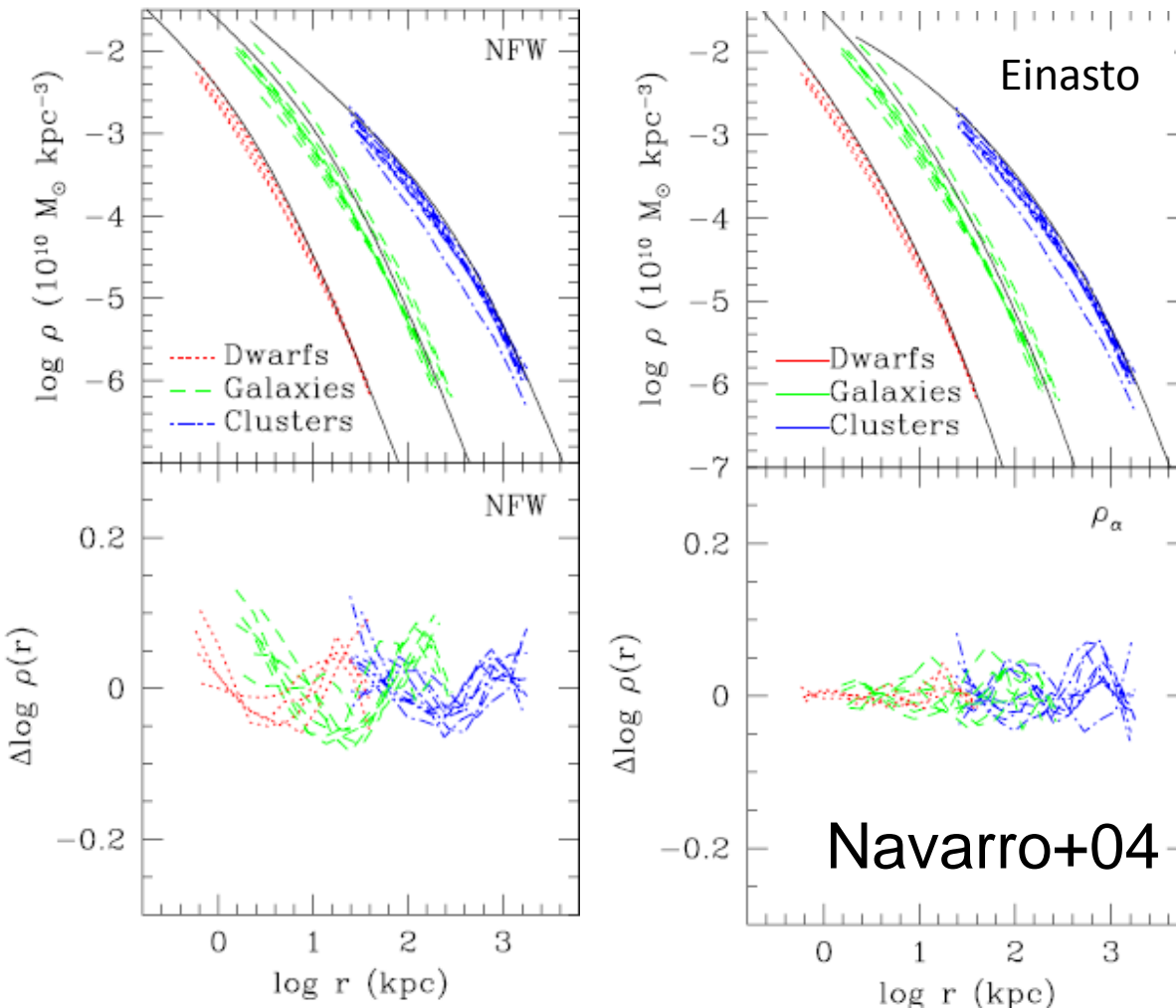
Geometric area
distortion



n/μ

“Diversity” of halo density profiles

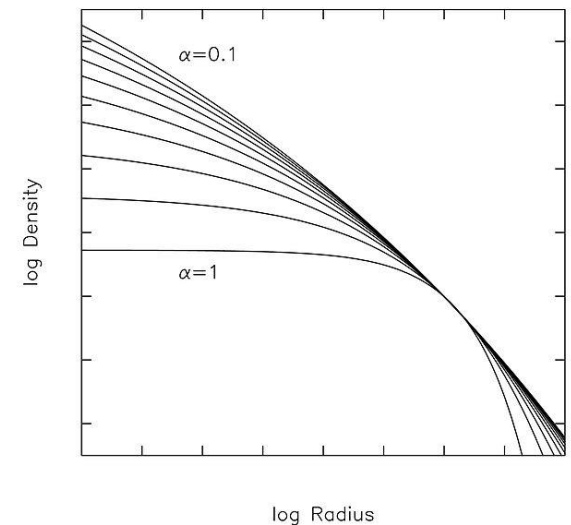
Mass profiles of DM halos are not strictly self-similar:



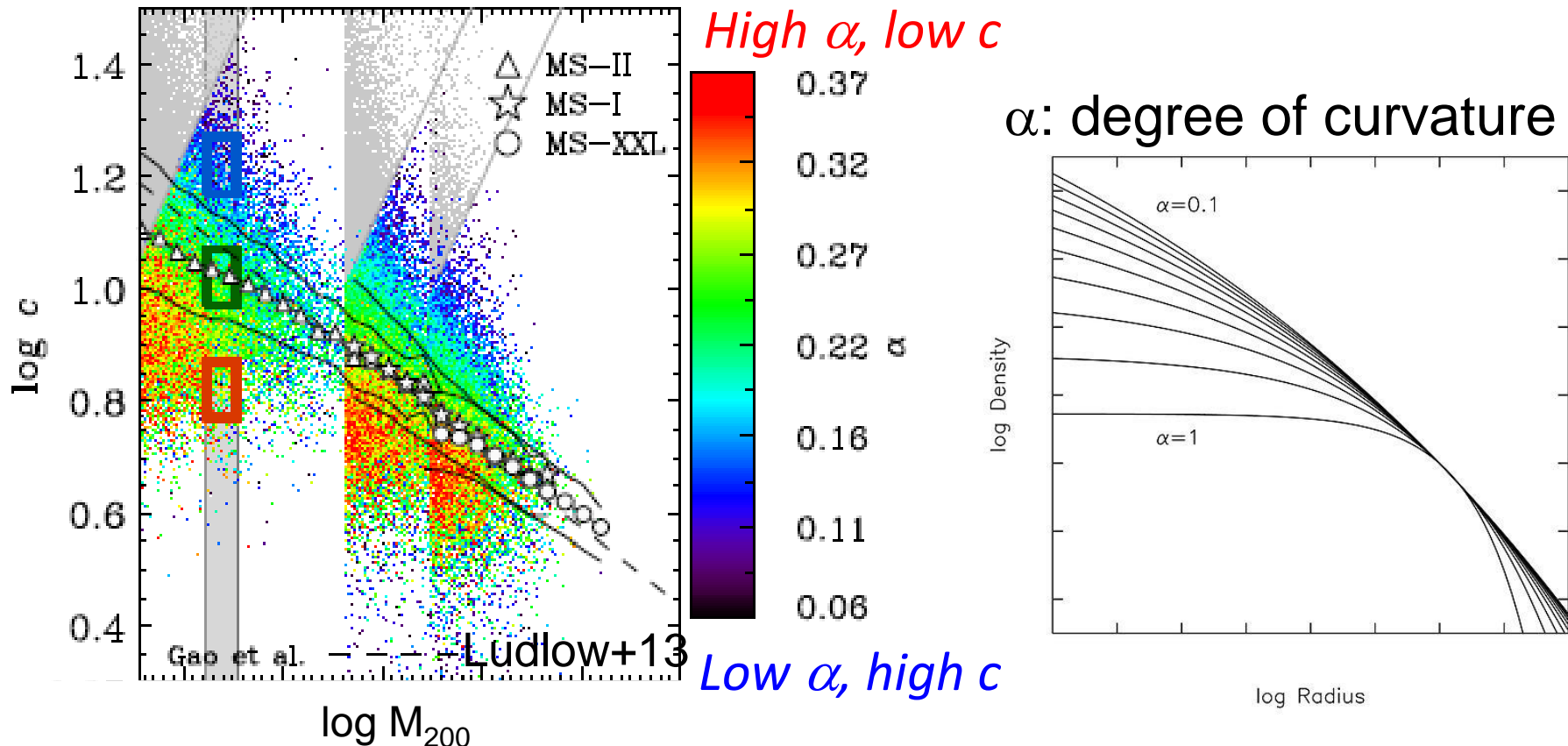
Einasto profile (ρ_s, r_s, α)

$$\frac{d \ln \rho(r)}{d \ln r} = -2 \left(\frac{r}{r_s} \right)^{\alpha}$$

α : degree of curvature



Intrinsic Scatter in $c(M)$: Mass Assembly Histories (MAH)



High α , low c

Low α , high c

α : degree of curvature

- Scatter is due to another DoF (α), related to MAH (Ludlow+13)
- Larger or smaller values of α correspond to halos that have been assembled more or less rapidly than the NFW curve
- Clusters with average c_{200} have the NFW-equivalent $\alpha \sim 0.18$

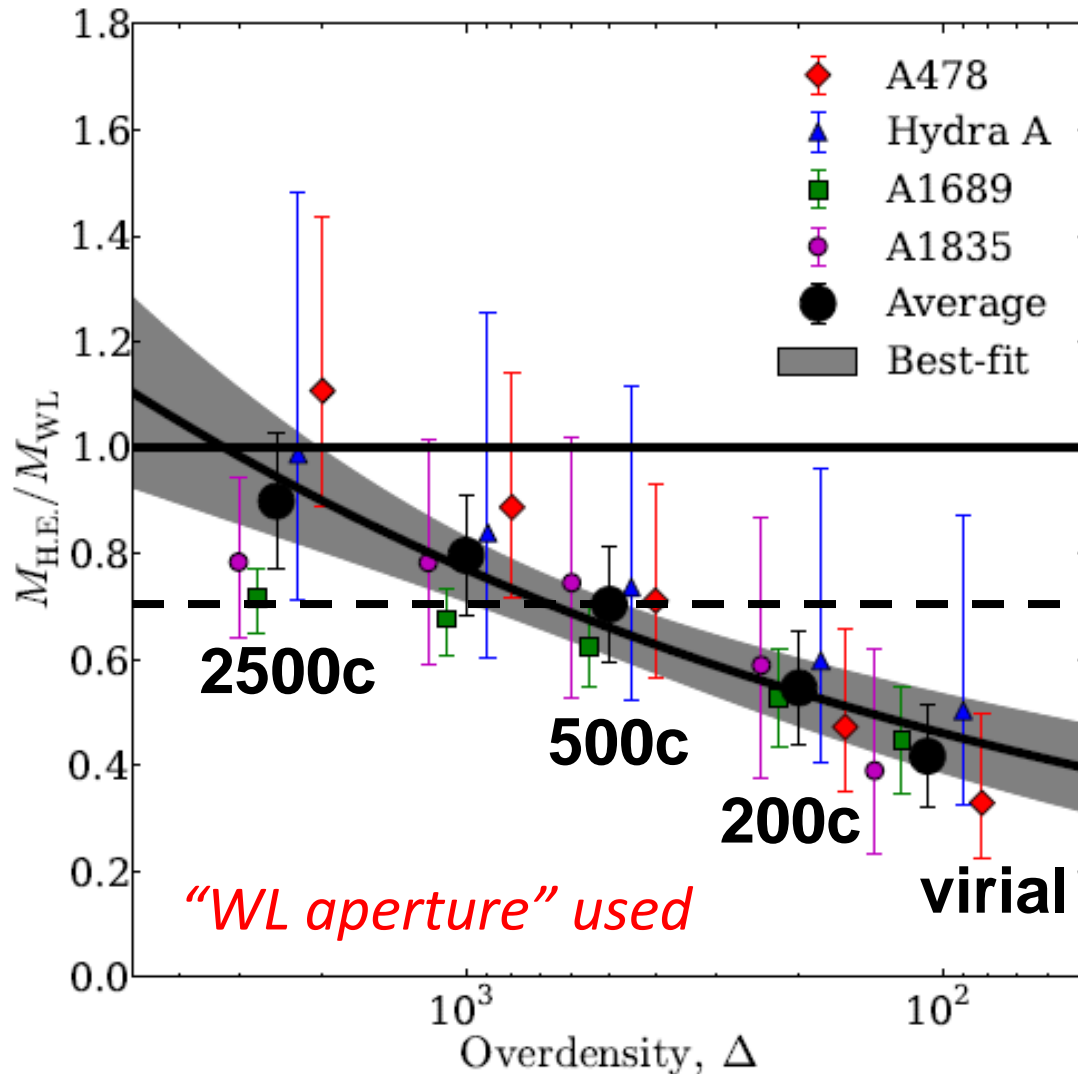
$$\begin{aligned}
ds^2 &= a^2(\eta)d\tilde{s}^2 = a^2\tilde{g}_{\mu\nu}dx^\mu dx^\nu \\
&= a^2 \left[-(1+2\Psi)d\eta^2 + (1-2\Psi) \left\{ d\chi^2 + r^2(\chi)(d\theta^2 + \sin^2\theta d\phi^2) \right\} \right]
\end{aligned}$$

$$\delta k^\mu(\lambda) = -\frac{2}{r^2(\lambda)} \int_0^{\lambda_s} d\lambda' \partial^\mu \Psi(\lambda') / c^2 \quad (\mu = \theta, \phi).$$

$$\beta - \theta = \int_{\text{Observer}}^{\text{Source}} d\alpha = \alpha(\chi_s),$$

$$\alpha(\chi_s) = -\frac{2}{c^2} \int_0^{\lambda_s} d\lambda \frac{r(\lambda_s - \lambda)}{r(\lambda_s)} \nabla_\perp \Psi(x(\lambda)); \quad x(\lambda) = x^{(b)}(\lambda) + \delta x(\lambda)$$

Suzaku-X HSE vs. Subaru WL

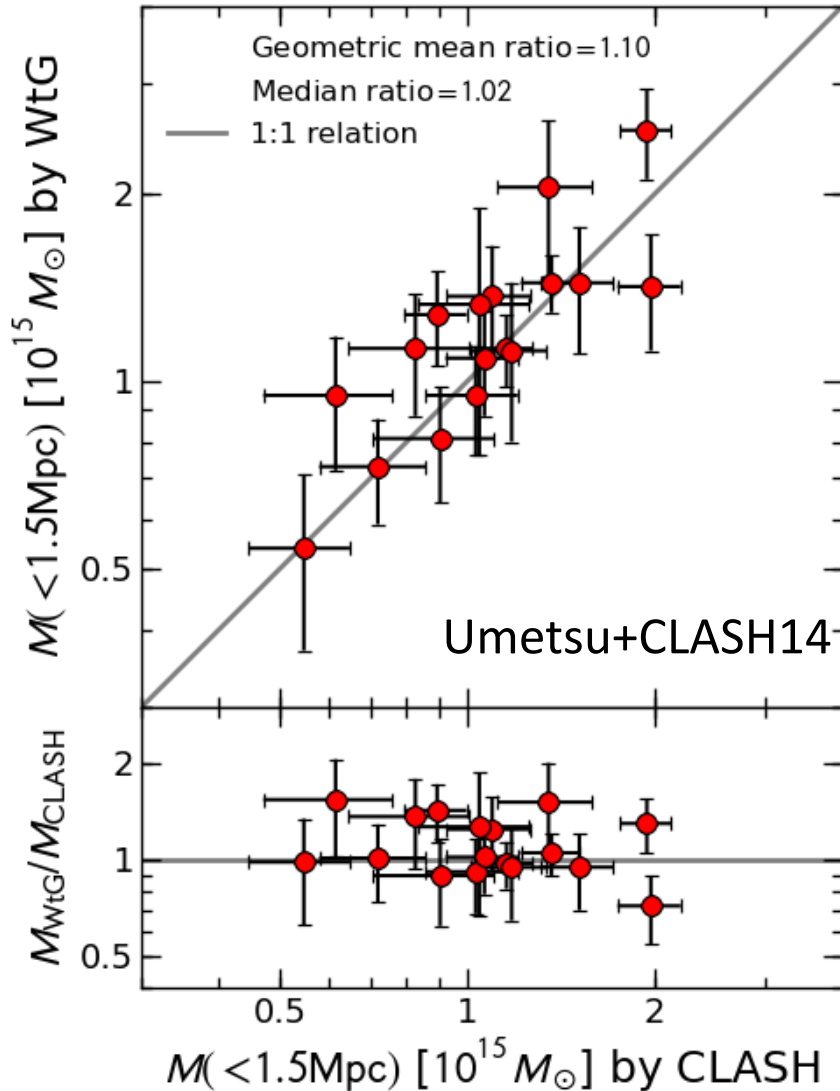


Independent *Suzaku*-HSE vs. Subaru-WL results, consistent with XMM-HSE vs. Subaru-WL of CLASH collaboration

Okabe, Umetsu et al.14, PASJ, in press (arXiv:1406.3451)



Comparison with WtG @R=1.5Mpc



17 clusters in common (Subaru):

- **WtG**: shear-only (Applegate+14), NFW $c_{200c}=4$ prior
- **CLASH**: shear + magnification, NFW log-uniform: $0.1 < c_{200c} < 10$

Un-weighted geometric mean mass ratio ($\langle Y/X \rangle = 1/\langle X/Y \rangle$)

- $\langle M_{\text{WtG}}/M_{\text{CLASH}} \rangle = 1.10$
- Median ratio = 1.02

Systematic uncertainty in the overall mass calibration of 8% from shear-magnification consistency (Umetsu+14)

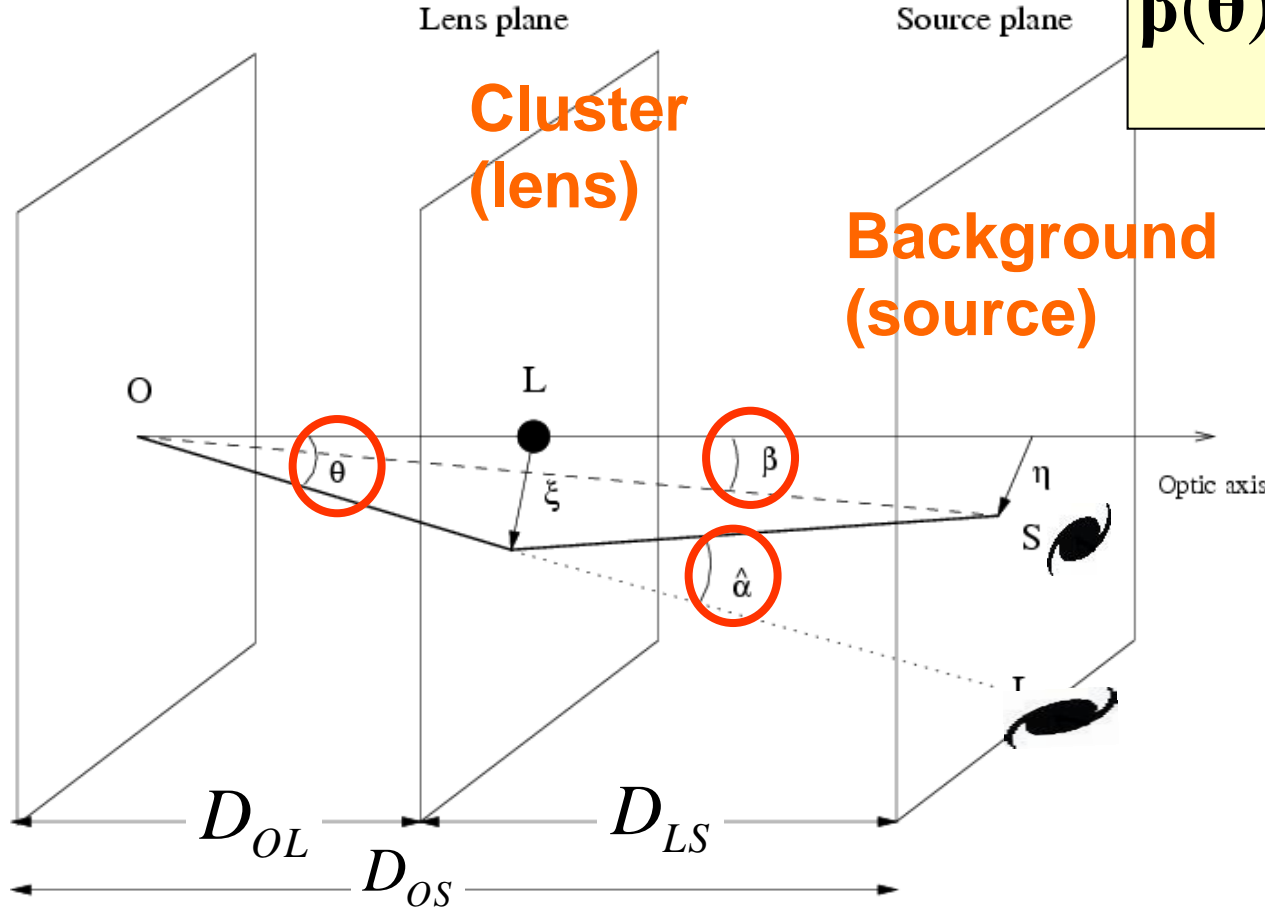
No mass dependent bias

Cluster Lens Equation

Cosmological lens equation + single/thin-lens approximations

β : true (but unknown) source position

θ : apparent image position



$$\beta(\theta) - \theta = \frac{D_{LS}}{D_{OS}} \int \delta \hat{\alpha}(\theta)$$

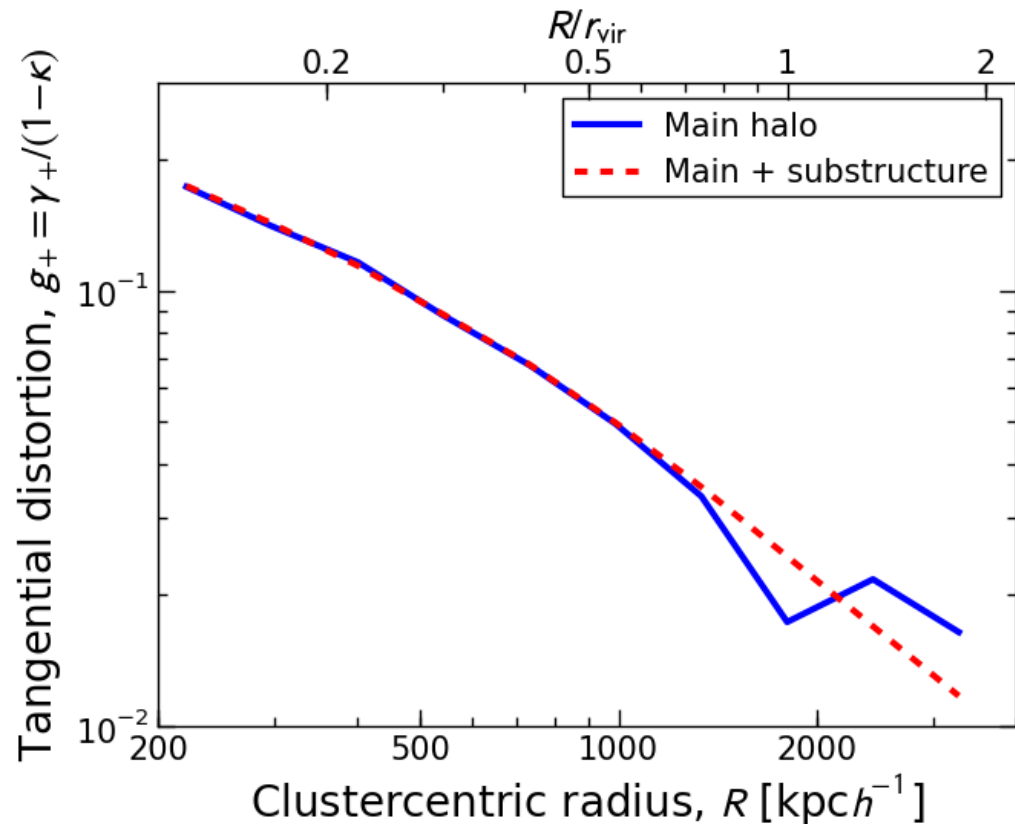
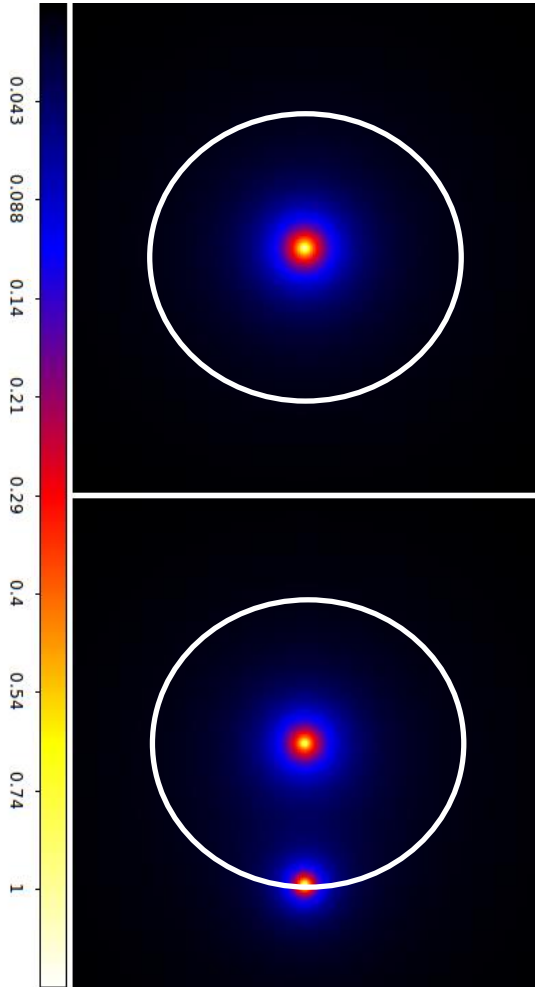
Angular diameter distances:

$$D_{OL}, D_{LS}, D_{OS} \sim O(c/H_0)$$

For a rigid derivation of cosmological lens eq., see, e.g., Futamase 95

Non-local substructure effect

A substructure at $R \sim r_{\text{vir}}$ of the main halo, modulating $\Delta\Sigma(R) = \Sigma(< R) - \Sigma(R)$

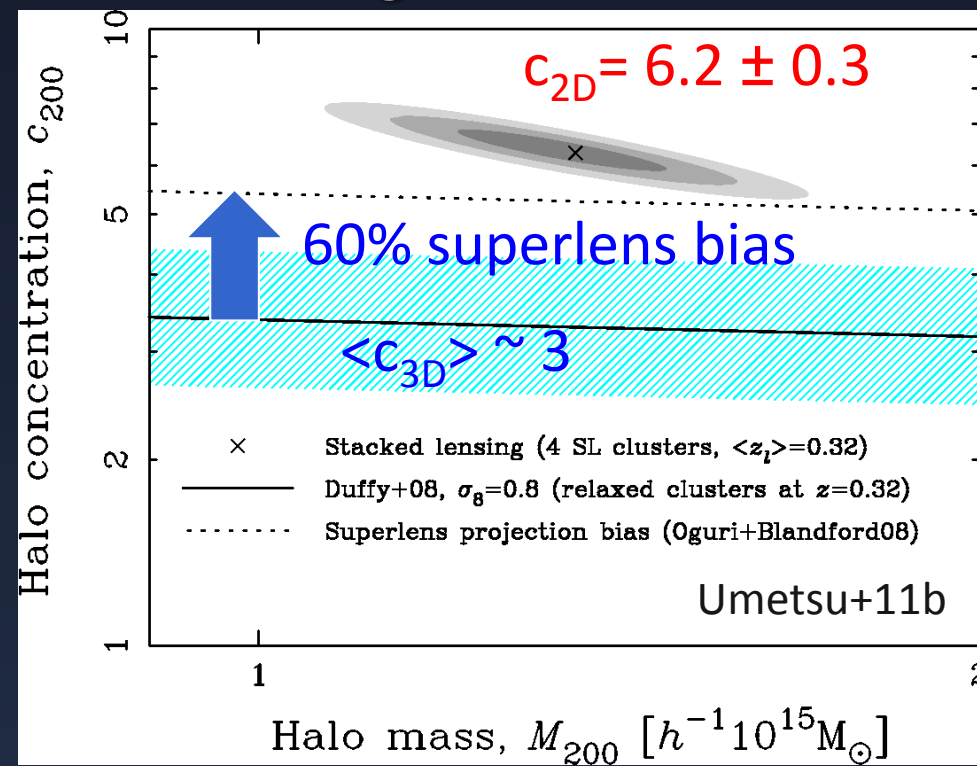
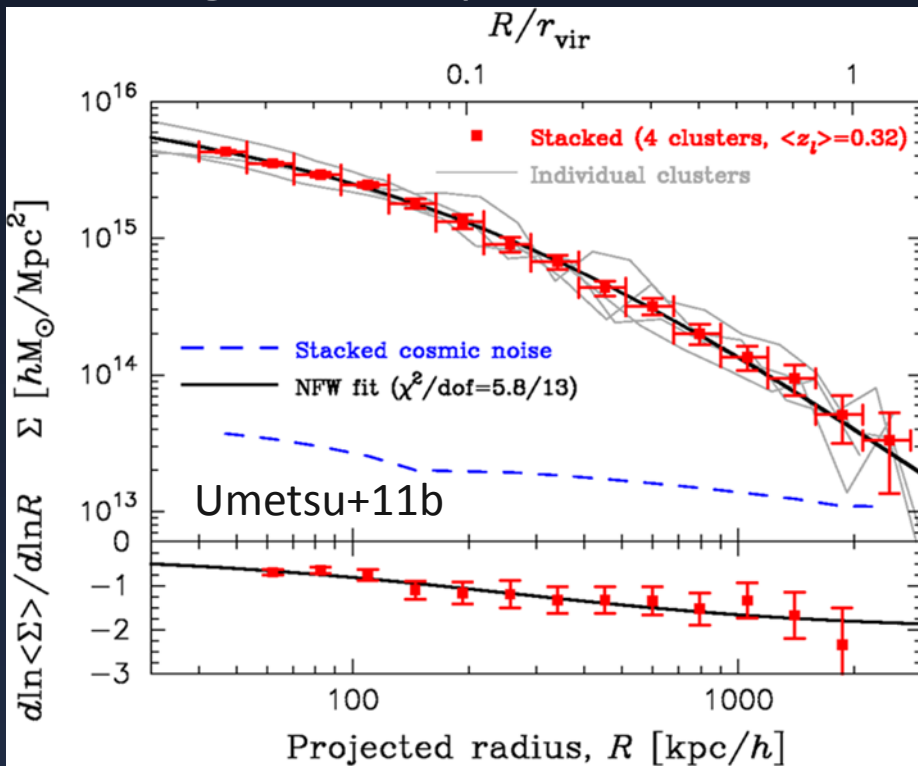


Known $\sim 10\%$ negative bias in mass estimates from tangential-shear fitting, inherent to clusters sitting in substructured field (Rasia+12)

CLASH Objectives & Motivation

$$c_{200c} := \frac{r_{200c}}{r_s}$$

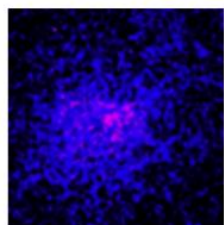
Before CLASH (2010), deep-multicolor Strong (*HST*) + Weak (Subaru) lensing data only available for a handful of **strong-lens clusters**



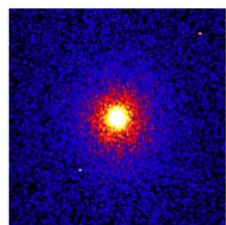
Total mass profile shape: consistent w CDM (self-similar universal profile)

Degree of concentration: maximum superlens correction not enough if $\langle c_{\text{LCDM}} \rangle \sim 3$?

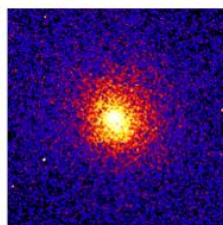
X-ray observations with Chandra and XMM-Newton Satellites



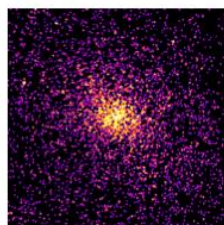
Abell 209



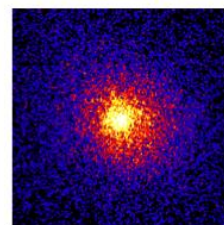
Abell 383



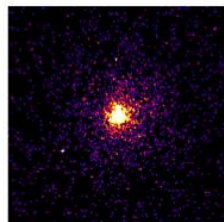
Abell 611



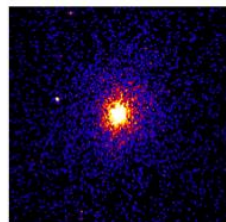
Abell 1423



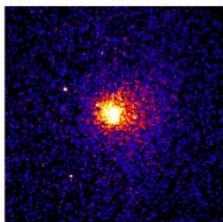
Abell 2261



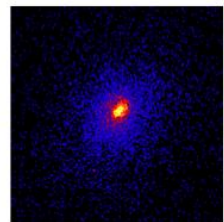
MACS 0329-0211



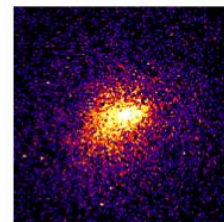
MACS 0429-0253



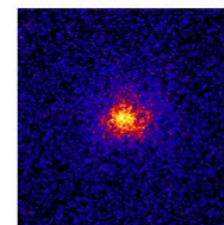
MACS 0744+3927



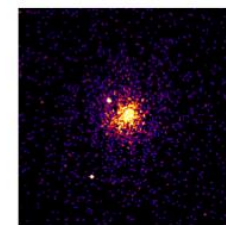
MACS 1115+0129



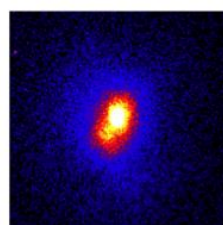
MACS 1206-0847



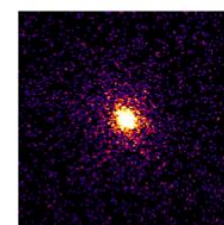
CLJ1226+3332



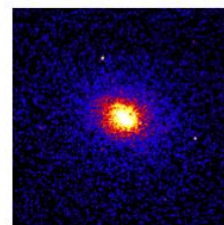
MACS 1311-0310



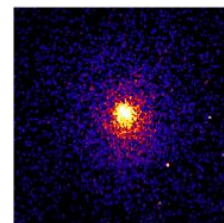
RXJ 1347-1145



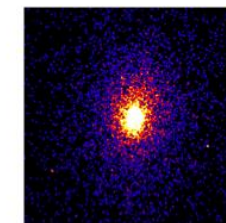
MACS 1423+2404



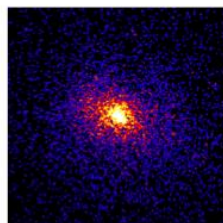
RXJ 1532+3020



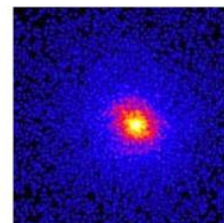
MACS 1720+3536



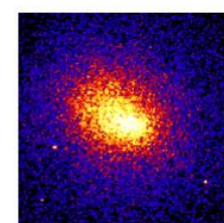
MACS 1931-2634



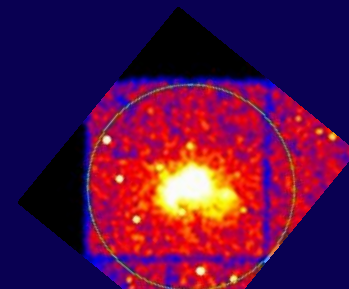
RXJ 2129+0005



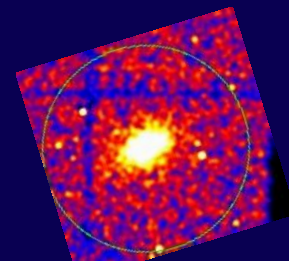
MS-2137



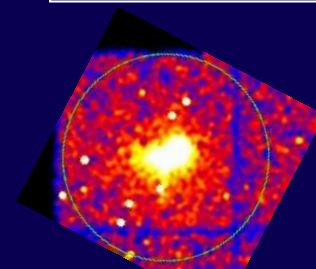
RXJ 2248-4431



MACS 0717+3745



RXJ 0647+7015



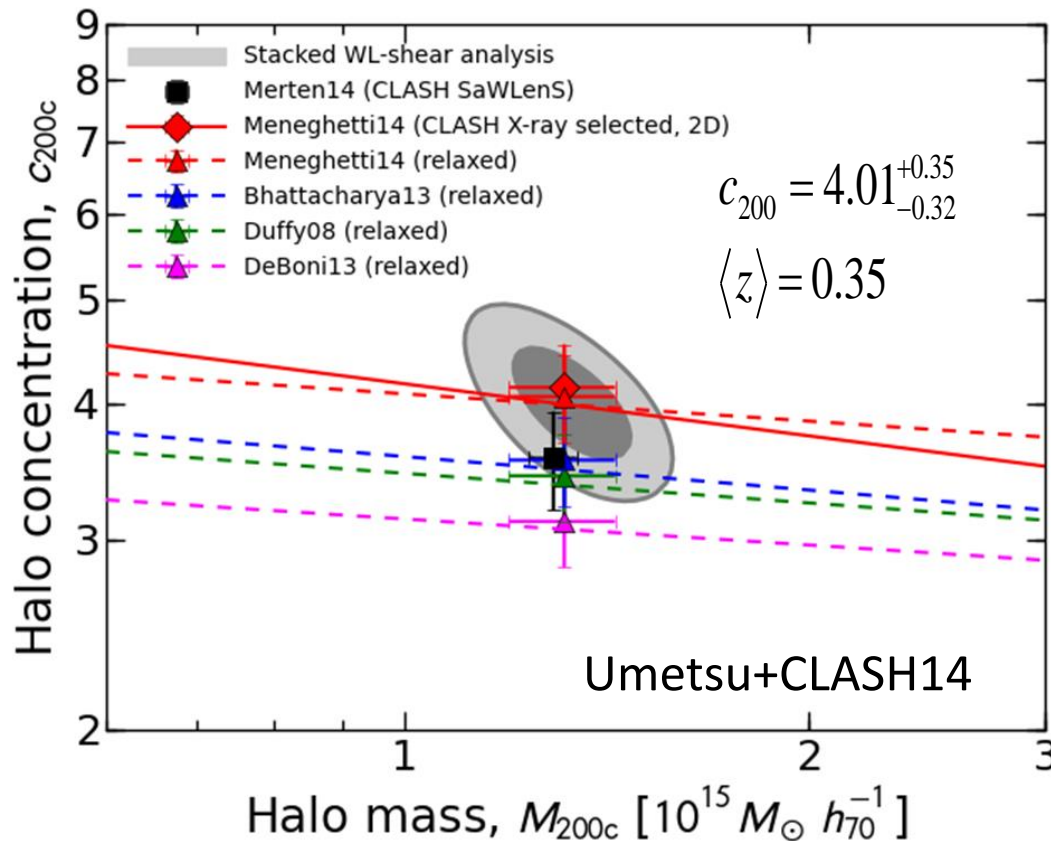
MACS 1149+2223

All have
 $T_x > 5$ keV

X-ray images of 23 of the 25 CLASH clusters. 20 are selected to be “relaxed” clusters (based on their x-ray properties only). 5 are selected specifically because they are strongly lensing $\theta_E > 30''$



CLASH-WL vs. c-M relations



M14 (CLASH): $\sigma_8 = 0.82$

Bhat13: $\sigma_8 = 0.8$

Duffy08: $\sigma_8 = 0.8$

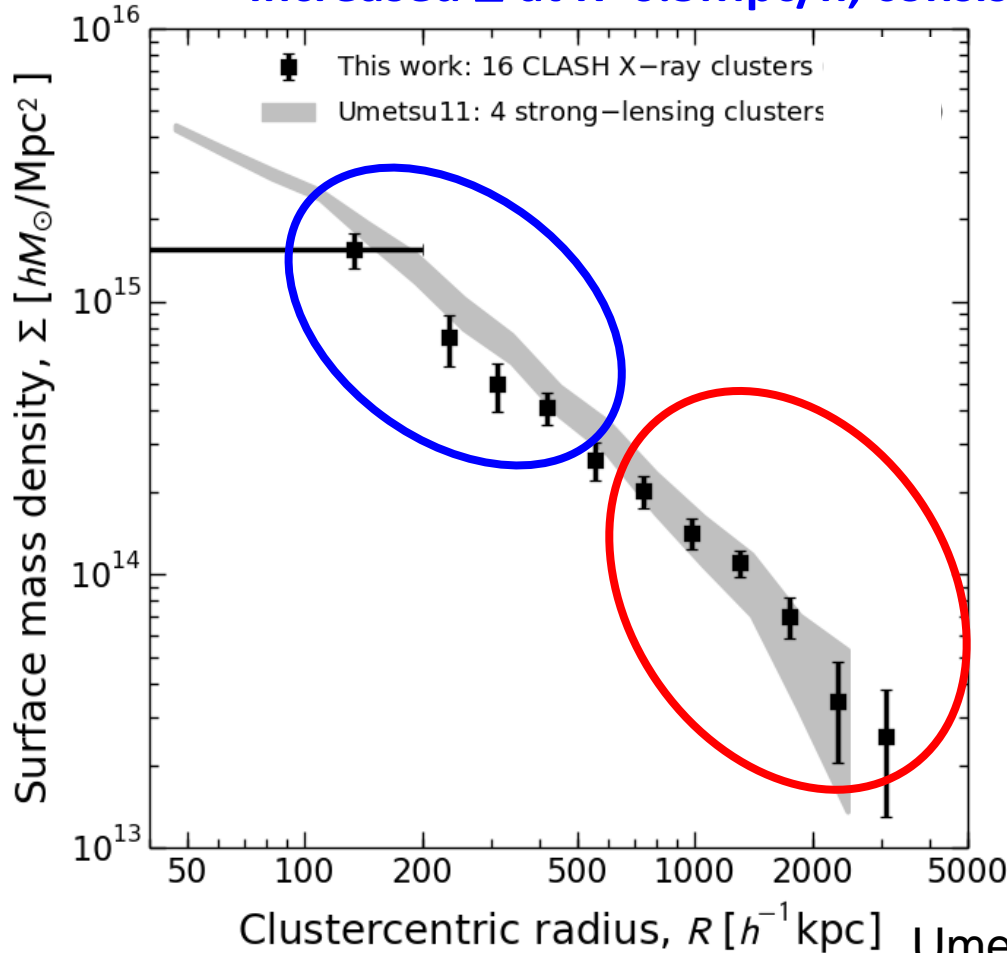
DeBoni13: $\sigma_8 = 0.78$

At low M_{200c} , X-ray selection picks up clusters with higher concentrations (Meneghetti+14)



Comparison with pre-CLASH results

- C_{200} vs θ_E relation, consistent with triaxial CDM halos (Oguri+12)
- **Similar v (MAH), similar Σ in outskirts (Diemer & Kravtsov 14)**
- **Increased Σ at $R < 0.5 \text{ Mpc}/h$, consistent w orientation bias (Gao+12)**



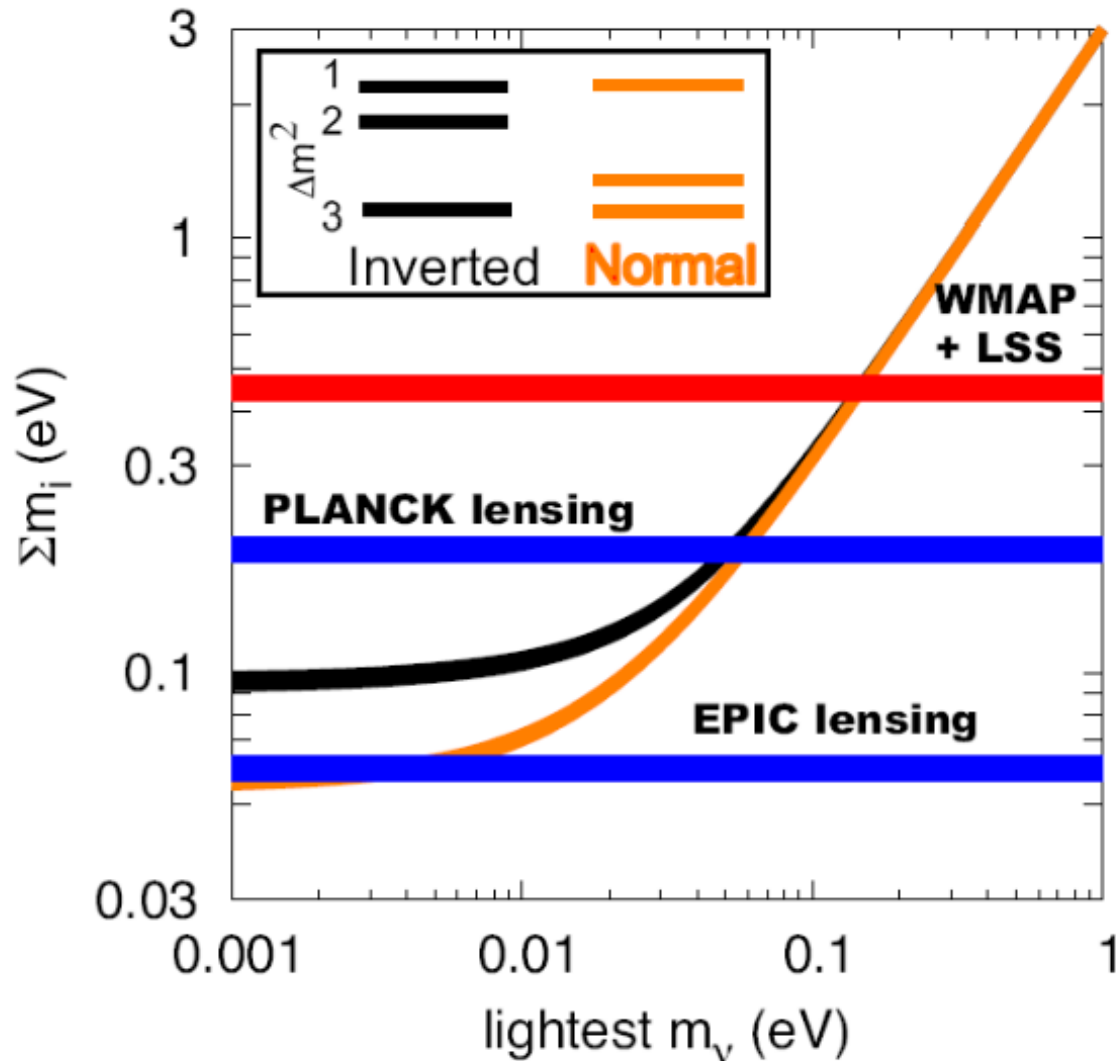
CLASH X-ray-selected sample

- $M_{200} = 1.3e15 M_{\text{sun}}$
- $\underline{C_{200} = 4.0}$
- $\underline{\theta_E \sim 15''}$ ($z_s = 2$)
- $\underline{v = 3.8}$ ($b_h \sim 9$)

Umetsu11b sample

- $M_{200} = 1.7e15 M_{\text{sun}}$
- $\underline{C_{200} = 6.1}$
- $\underline{\theta_E \sim 36''}$ ($z_s = 2$)
- $\underline{v = 4.1}$ ($b_h \sim 11$)

Neutrino Mass Hierarchy from Cosmology



Future Cosmological Constraints on Neutrino Hierarchy

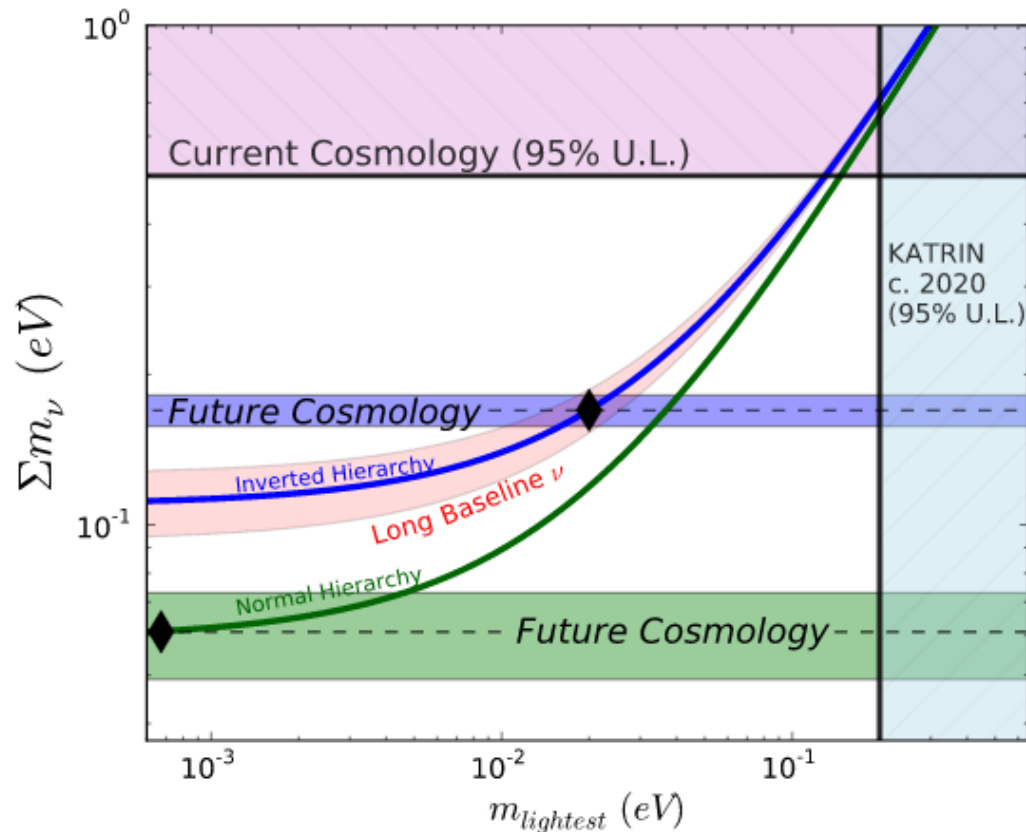


Figure 1-2. Shown are the current constraints and forecast sensitivity of cosmology to the neutrino mass in relation to the neutrino mass hierarchy. In the case of an “inverted hierarchy,” with an example case marked as a diamond in the upper curve, future combined cosmological constraints would have a very high-significance detection, with 1σ error shown as a grey band. In the case of a normal neutrino mass hierarchy with an example case marked as diamond on the lower curve, future cosmology would detect the lowest Σm_ν at a level of $> 4\sigma$.